Geomechanics and Engineering, *Vol. 42, No. 2 (2025) 147-168*
https://doi.org/10.12989/gae.2025.42.2.147

Numerical analysis study for estimating the freezing range of tunnels in cold regions

Hwan-Hee Yoon[1a], Young-Su Kim[1b], Ha-My Tran[2c], Joon-Shik Moon[3d] and Hyuk-Sang Jung*[2]

[1]*KECC, Korea Engineering Consultants Corp. Institute of Technology, 21 Sangil-ro 6-gil Gangdong-gu, Seoul 05288, Republic of Korea*
[2]*Dongyang University, Dept. of Railroad Construction and Safety Engineering, 145 Dongyangdae-ro, Punggi-eup, Yeongju-si, Gyeongsangbuk-do 36040, Republic of Korea*
[3]*Kyungpook University, Dept. of Civil Engineering,80 Daehak-ro, Buk-gu, Daegu, Republic of Korea*

(*Received August 1, 2023, Revised May 22, 2025, Accepted June 7, 2025*)

Abstract. This study presents a numerical analysis approach to determine the freezing range of tunnels in cold regions. The analysis utilizes numerical methods to analyze the temperature distribution inside the tunnel and the temperature distribution of the surrounding ground. Based on the numerical analysis results, a regression equation is proposed to estimate the freezing range. In South Korea, more than 70% of the land consists of mountainous areas, leading to an increasing trend in tunnel construction due to limited land availability for road and railway development. Consequently, the importance of maintenance and management of tunnel structures has been emphasized. Tunnels operating in cold regions, particularly in well-known areas like Gangwon Province, are susceptible to freezing-related damages such as icicle formation, ice accumulation, and blockage of drainage pipes. Therefore, this study aims to determine the freezing range of tunnels in cold regions using numerical analysis methods. The research findings confirm the temperature distribution inside the tunnel and the ground surrounding the tunnel under various structural and environmental conditions. By utilizing the results of the numerical analysis, regression equations are derived to estimate the freezing rate along the longitudinal direction of the tunnel and the depth of ground freezing around the tunnel. These research outcomes can serve as a useful indicator for assessing the freezing prevention measures and facilitating efficient maintenance and management of tunnels in cold regions.

Keywords: cold region; freezing range; heat transfer analysis; tunnel freezing

1. Introduction

The Daegwallyeong area in Gangwon Province of South Korea records the lowest average winter temperatures, reaching -5.3°C, while the average temperature for the entire Gangwon Province is -1.73°C. Furthermore, the lowest temperatures in the winter in the Gangwon area are recorded in the Daegwallyeong area, with a minimum temperature of -10.5°C, and the average lowest temperature for the entire Gangwon Province is -6.7°C. China, which is adjacent to South Korea, classifies regions with an average temperature of 0°C to 10°C during the coldest month, with daily average temperature below 5°C, and a heating period of 90 to 145 days as cold regions. If China's classification for cold regions is applied, all areas in the Gangwon Province, except Donghae City, would fall into the cold region category (Jun, 2019).

In South Korea, due to the country's mountainous terrain and environmental challenges, the construction of tunnels has been increasing. According to the Ministry of Land, Infrastructure and Transport's report on road bridges and tunnels (2020), the number of road tunnels increased by 116 to a total of 2,682 in 2019 compared to the previous year, marking an overall increase of 1,300 tunnels over the past decade. Among them, there are 399 operational road tunnels in the Gangwon Province. Furthermore, according to the statistics from the Ministry of Land, Infrastructure and Transport (2020), there are a total of 844 operational railway tunnels in the country, including 134 for high-velocity railways and 710 for conventional railways.

Despite the large number of tunnels in operation, there cases of freezing damage have been reported during severe winter cold spells. Typical freezing damages in tunnels include the formation of icicles and ice dams due to freezing at construction joints, blockage of drainage pipes due to freezing, and icing on road surfaces and railway tracks. There types of freezing damages can be attributed to inadequate design considerations, drainage system failures due to frozen pipes, and potential accidents involving vehicles and trains. These issues directly impact the stability of tunnels and the safety of vehicle and train operations, necessitating effective countermeasures.

In response to the risk of tunnel freezing damage, various anti-freezing methods are being applied in South Korea. However, in tunnel design standards, there is a guideline stating that in cases where freezing is a concern,

*Corresponding author, Professor
E-mail: yoricom@dyu.ac.kr
[a]Ph.D.
[b]Ph.D.
[c]Ph.D. Student
[d]Professor

ISSN: 2005-307X (Print), 2092-6219 (Online)

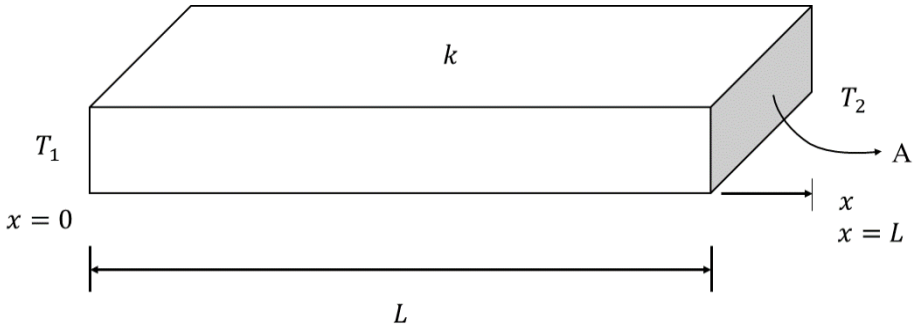

Fig. 1 Heat conduction in a cuboid (Kang *et al*. 2013)

measures to prevent icing in drainage systems should be considered. Nevertheless, there is no specific explanation regarding the scope of application for anti-icing methods based on the tunnel's structure and environmental conditions.

Although there have been numerous studies on internal temperature measurement in currently operating tunnels, Park *et al.* (2022) and Moon *et al.* (2022) analyzed and predicted the effects of freezing on tunnel structures, and Jin *et al.* (2022) and Assel *et al.* (2021) studied freeze-thaw cycles and frost load tests. However as well as analyses of insulation performance and the insulation effect based on the thickness of insulation materials, there is still a lack of research that considers the structural and environmental conditions of tunnels to predict the freezing range of tunnels and provide guidelines for the application range of anti-freezing methods. Therefore, it is necessary to analyze the temperature distribution inside tunnels and the surrounding ground considering the structural and environmental conditions and predict the freezing range to determine appropriate anti-freezing methods.

Therefore, this study aims to estimate the freezing range in tunnels in cold regions by conducting a three-dimensional numerical analysis of heat transfer considering the structural and environmental conditions. Based on the analysis results, a regression equation is proposed to predict the freezing range in tunnels and provide suggestions for the application scope of anti-freezing methods. The findings of this study are expected to contribute to the stability of tunnels and the safety of vehicle and train operations.

2. Theoretical background

2.1 Theory of heat transfer

The theory of heat transfer in a tunnel involves the transfer of thermal energy between the tunnel and its surroundings. This process can occur through three mechanisms: conduction, convection, and radiation.

(1) Conduction

Conduction refers to the direct transfer of heat between objects or substances through direct contact. In the case of a tunnel, conduction mainly occurs between the tunnel walls and the surrounding soil or rock. Thermal conductivity controls conduction and can be expressed by Fourier's law of heat conduction, as shown in Fig. 1 and Eq. (1)

$$q = -kA\frac{dT}{dx} = kA\frac{T_1 - T_2}{L} \quad (1)$$

Where q is the heat flux (W/m^2), k is the thermal conductivity (W/m·K), A is the cross-sectional area (m^2), $\frac{dT}{dx}$ is the temperature gradient (K/m).

(2) Convection

Convection involves the transfer of heat through the movement of fluids, such as air or water. In the context of a tunnel, convection occurs when there is air movement inside the tunnel or when air flows over the tunnel surfaces. The rate of convective heat transfer can be described by Newton's law of cooling (Eq. (2)), given by

$$q = hA(T_s - T_\infty) \quad (2)$$

Where h is the convection coefficient (W/m^2·K), T_s is the temperature of the tunnel surface (K), T_∞ is the temperature of the surrounding fluid (K).

(3) Radiation

Radiation refers to the transfer of heat energy through electromagnetic waves. In the case of a tunnel, radiation occurs between the tunnel surfaces and the surrounding environment. The rate of radiative heat transfer can be calculated using the Stefan-Boltzmann law (Eq. (3)), given by:

$$q = \varepsilon\sigma A T_s^4 \quad (3)$$

Where ε is the emissivity, σ is the Stefan-Boltzmann constant, A is the surface area (m^2), T_s is the temperature of surface (K).

It's important to note that these three mechanisms of heat transfer can occur simultaneously and their contributions to the overall heat transfer in a tunnel depend on various factors such as the thermal properties of the materials involved, air movement, and temperature differences.

2.2 Cases of tunnel frost damage

According to the Korea Expressway Corporation (2013), it has been observed that if the average daily temperature at

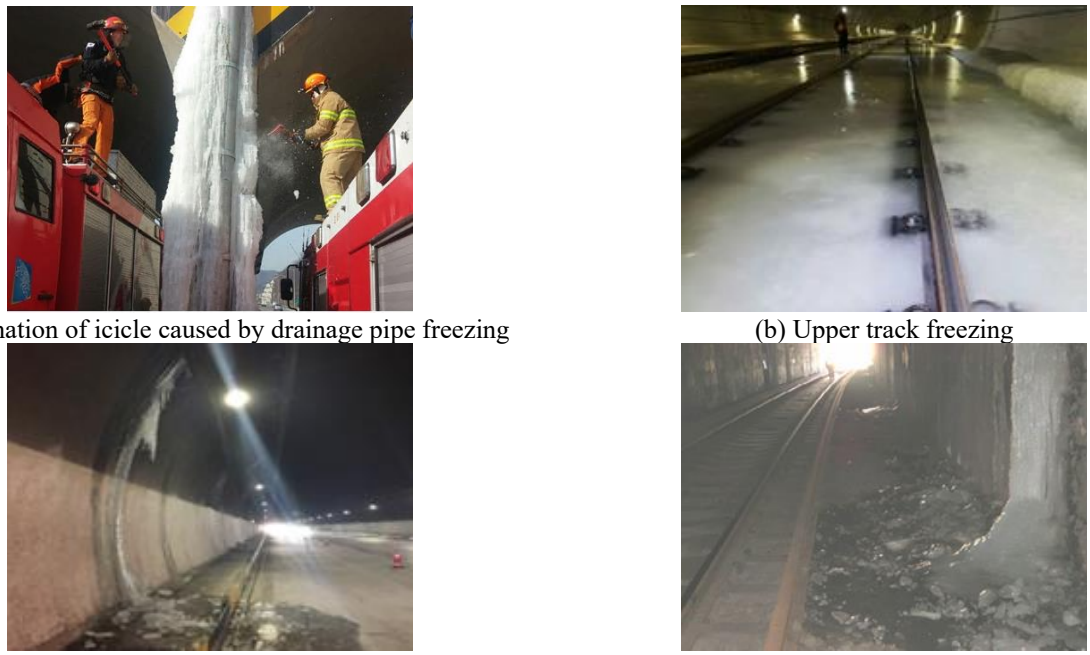

(a) Formation of icicle caused by drainage pipe freezing (b) Upper track freezing

(c) Freezing caused by wall leakage (d) Freezing caused by lining crack

Fig. 2 Cases of tunnel freezing damage (An 2020, Zhao *et al*. 2020, Cui and Wang 2021)

the Daegwallyeong 1 Tunnel remains below approximately -7°C for 2-3 consecutive days, the drainage pipes freeze, and icicles form from the floor to the ceiling at the construction joints. Furthermore, it has been confirmed that Sorae Tunnel experiences repeated freezing and leakage of drainage pipes during winter, leading to repetitive maintenance work. The Korea Expressway Corporation (2006) reported incidents of drainage pipe blockage due to freezing at the entrance of Dunnae Tunnel up to 200 m, as well as at the entrance of Bongpyeong Tunnel up to 300 m. Additionally, Hwang (2013) identified damages caused by freezing in seven tunnels in the Gangwon area, including cracks and deformations due to freezing, pavement thawing, leaks due to cracks in the concrete lining, blockage of drainage pipes, and icicle formation. In a tunnel in Seoul, icicles measuring over 600 mm were formed on the ceiling near the tunnel entrance and pedestrian pathway, resulting in a 10-car collision accident when the icicles fell onto vehicles. In another tunnel in Gwangju, a drainage pipe installed at a height of approximately 5 m from the tunnel entrance froze, causing icicle formation (An 2020). In the case of railway tunnels, the Dunnae Tunnel on the Wonju-Gangneung Line experienced track freezing on the upper part of the track due to the freezing of drainage facilities in the tunnel's 300 m section.

In China, leaks occurred on the tunnel sidewalls at the 1,825 m point from the tunnel entrance in the Xinganling Tunnel, and ice formation was observed on the tunnel sidewalls at the 1,450 m point from the entrance (Zhao *et al*. 2020). Furthermore, in another tunnel in China, cracks and leaks caused by freezing were observed on the tunnel sidewalls (Ma *et al*. 2018). Chinese railway tunnels experienced the freezing of drainage pipes leading to the freezing of the upper part of the track, as well as ice formation due to leaks from cracks in the lining sidewalls (Cui and Wang 2021). Fig. 2 displays cases of tunnel freezing damage.

2.3 Tunnel freezing design standards

In order to analyze the freezing criteria for domestic tunnels, various standards related to tunnel, road, and railway design, as well as standard construction specifications, were investigated. The results of the investigation revealed that the criteria for freezing in domestic tunnels are only mentioned in the drainage and waterproofing standards for tunnel design (KDS 27 50 05, 2016), which state that "Measures to prevent freezing in drainage systems should be established in cases where freezing, such as in tunnel portal, is a concern." However, the tunnel design and construction standards and standard construction specifications for roads and railways do not provide specific criteria for tunnel freezing. It is stated that any unspecified matters should follow the tunnel design standards (KDS 27 00 00, 2018).

According to the design standards in Japan regarding tunnel freezing damage, it is explicitly stated that in cold regions, insulation should be installed between the waterproofing sheet and the lining of road and railway tunnels to prevent frost and icicle formation, as it can lead to vehicle accidents. The use of insulation is mentioned for the purpose of ground freezing prevention in cold regions. Additionally, in extreme climates, tunnels need to consider factors such as length, prevailing wind direction, and wind velocity. Specifically, within a 100m section near the portal, where temperatures decrease rapidly, it is specified that insulation material design should be performed, and the thickness of insulation materials should be determined based on thermal conductivity analysis (Korea Expressway Corporation 2013).

Table 1 The guidelines for preventing tunnel freezing in Norway (Broch *et al.* 2002)

Method of W&FPS :	Tunnel Class (AADT)				
	A (<2500)	B (2500~5000)	C (5000~10000)	D (10000~15000)	E (>15000 two tubes)
WG-Tunnel fabric, not insulated	○[1]				
Miljohvelv, insulated (metal sheet W&FPS)	●	●	○[2]		
PE-foam w/60 mm sprayed concrete, steel fibres	●	●			
PE-foam w/60 mm sprayed concrete, mesh reinforced	●	●	●*	●*	●*
Concrete Elements	●	●	●	●	●
Cast concrete with membrane	●	●	●	●	●

○[1]= may be used up to AADT 1000(Annual Average Daily Traffic) and below a given frost limit(F10T < 20000h˚C).

○[2]= concept is modified for tunnel class C.

●*= concrete wall elements must normally be used

According to Broch *et al*. (2002), in Norway, when establishing anti-freezing measures, factors such as traffic volume, design velocity, tunnel length, tunnel cross-section, freezing index, maintenance, and cost-effectiveness are taken into consideration in the planning process. It is specified that Polyethylene foam (PE foam) should be used to prevent freezing in tunnel linings. Furthermore, it is reported that a thickness of 45 mm is considered appropriate for PE foam when the freezing index is up to 625°C·day. The Norwegian specifications for PE foam are presented in Table 1.

It has been observed that foreign countries provide relatively specific information regarding tunnel freezing compared to domestic guidelines. In the case of Japan, freezing prevention measures suitable for each region are presented with detailed justifications. In Norway, it has been found that research on tunnel freezing has been conducted for a long time. However, it is evident that there is a lack of information regarding the freezing range taking into account the structural and environmental conditions of tunnels.

2.4 Literature review

Kim *et al*. (2011) conducted temperature measurements to establish insulation measures for a cold region tunnel. They selected Hwaak Tunnel in Gapyeong, Gyeonggi Province as their subject and measured the temperature distribution according to the tunnel's end length. According to the measurements, the temperature at a distance of 30 meters from the tunnel entrance, at a depth of 200 mm inside the tunnel lining, decreased to -2℃ to -8℃.

Jun (2019) conducted an investigation on the internal temperature of multiple tunnels to analyze the characteristics of the internal temperature distribution and the correlation of factors that influence it. The study aimed to develop a calculation model for the internal temperature of tunnels, taking into account the factors that affect it. To conduct the research, Jun (2019) performed an internal temperature survey of road tunnels in Gangwon Province during the winter season. The survey employed on-site temperature measurements and long-term temperature monitoring methods. Additionally, considering the significant factors influencing the internal temperature, the study proposed a regression analysis-based model for calculating the internal temperature of tunnels.

Park *et al.* (2021) conducted temperature measurements to examine the variations in the internal temperature of a railway tunnel during winter train operations. They selected the ○○ Tunnel on the Gangneung Line as their target tunnel. The ○○ Tunnel is an 8,290-meter-long main tunnel located in the Gangwon region, where the outdoor temperature drops below -13℃, leading to freezing damage in the tunnel. Temperature measurements were taken along the longitudinal direction from the tunnel entrance to the midpoint at 3,270 meters. The results of the temperature measurements indicated that the internal temperature of the main tunnel gradually increased in a non-linear manner as it approached the center from the tunnel entrance. Additionally, it was analyzed that as the outdoor temperature decreased, the internal temperature of the tunnel also decreased, leading to the freezing of moisture and groundwater in the tunnel surroundings and an increase in the freezing damage zone.

Son *et al*. (2017) conducted a numerical analysis study to analyze the depth of frost penetration in road tunnels located in the cold region of Gangwon Province. The research findings indicated that caution is necessary regarding freezing damage when the tunnel ground is composed of bedrock. The depth of frost penetration showed an increasing trend as the subsurface temperature decreased. Therefore, the risk of freezing damage increases when the subsurface temperature of the tunnel's ground is lower. The study also mentioned that grounds consisting of sand are more susceptible to freezing compared to those composed of bedrock.

Wu *et al*. (2020) performed on-site measurements in a tunnel located in the eastern part of the Qinghai-Tibet Plateau in China to analyze temperature variations within the tunnel in a cold region. The measurement results

Table 2 Thermal properties of materials (Kim *et al.* 2011)

Division	Density (kg/m^3)	Specific Heat (J/kg·K)	Thermal Conductivity (W/m·K)	Viscosity (kg/m·s)
Air	1.225	1006.43	0.0242	1.7894e-05
Rock	2750	795.5	3.77	-
Concrete	2310	837.4	1.6	-

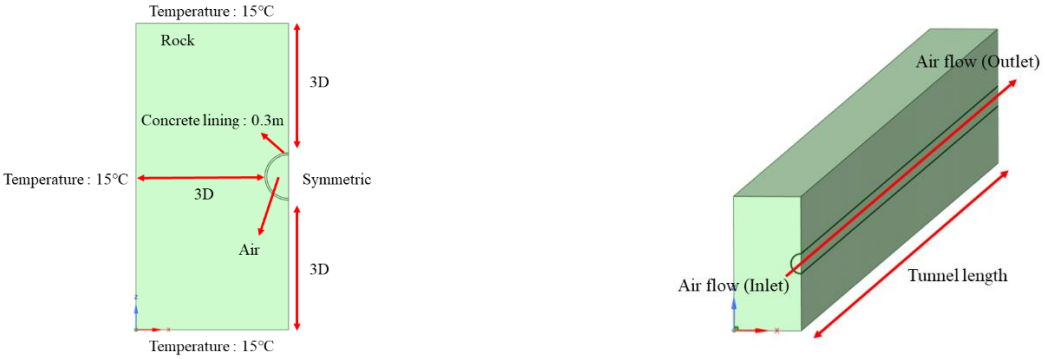

(a) 2D Modeling (b) 3D Modeling

Fig. 3 Tunnel modeling for heat transfer analysis

revealed that when the outdoor temperature was below freezing, the internal temperature distribution of the tunnel exhibited a pattern where the temperature increased from the tunnel entrance towards the central region and then decreased towards the tunnel exit. Furthermore, it was observed that the internal temperature distribution of the tunnel varied significantly depending on the wind velocity and wind direction.

Zhao *et al.* (2020) conducted temperature measurements on the tunnel ceiling, shoulder, and sidewalls at different lengths of the tunnel. They also measured the external temperature, wind velocity, and wind direction outside the tunnel. The distribution of internal temperatures within the tunnel exhibited a trigonometric function pattern over time, periodically changing with the outdoor temperature. The lowest recorded temperature within the tunnel was below -8°C. When sub-zero air from outside the tunnel entered through the tunnel entrance, the temperature increased gradually from the entrance towards the exit.

Zhou *et al.* (2016) analyzed the temperature distribution in a railway tunnel in cold regions, taking into account natural wind velocity, mechanical ventilation, and airflow generated during train operation. They compared and analyzed the results obtained from numerical calculations and on-site investigations to validate the accuracy of thetemperature distribution model in cold region railway tunnels.

Tao *et al.* (2022a) proposed a numerical heat transfer model for tunnels in cold regions and analyzed the effects of natural wind velocity, temperature, and mechanical ventilation on the temperature distribution within the tunnel. They also presented the relationship between tunnel freezing zones and the influencing factors. Additionally, Tao *et al.* (2022b) utilized a three-dimensional temperature calculation model to analyze the freezing zones within a tunnel in cold regions. They determined the length of freezing zones based on the tunnel's cross-sectional area and length.

3. Numerical analysis

3.1 Modeling

In order to determine the freezing range of a tunnel in a cold region, a three-dimensional numerical analysis was performed considering the structural and environmental conditions of the tunnel. When sub-zero ambient temperature infiltrates the tunnel, convection occurs in the concrete lining and the infiltrated air, while conduction occurs in the concrete lining and the surrounding ground. Therefore, a thermal analysis model that combines convection and conduction is required to determine the freezing range of the tunnel. In this study, numerical analysis was performed using Ansys Fluent, which can best simulate such a model.

The modeling for confirming the internal temperature of the tunnel and the temperature distribution of the lining and surrounding ground was composed of rock, concrete lining, and fluid (air). The shape of the tunnel was assumed to be circular, and a half-section modeling was performed considering the analysis time. The thickness of the concrete lining was set to 300 mm, and for the rock, the distance from the concrete lining to the left and upper/lower boundary surfaces was applied as three times (3D) the diameter of the tunnel cross-section. The thermal properties for the fluid, concrete lining, and rock were applied as shown in Table 2, and the flow of the fluid inside the tunnel was assumed to be turbulent flow. As for the boundary conditions, a subsurface temperature of 15°C was applied to

Table 3 Results of model validation

Tunnel length(m)	Temperature(°C)		Difference	
	Field measurement (A)	Numerical analysis (B)	Value (B-A)	Error (%)
0	-17.80	-16.44	1.36	7.63
30	-16.33	-15.19	1.14	6.97
100	-14.89	-14.82	0.07	0.47
170	-14.65	-14.57	0.08	0.58
250	-13.74	-14.40	-0.66	4.77
340	-13.98	-14.24	-0.26	1.86
650	-12.42	-13.55	-1.13	9.07
Average			0.09	4.48
Correlation coefficient			0.98	

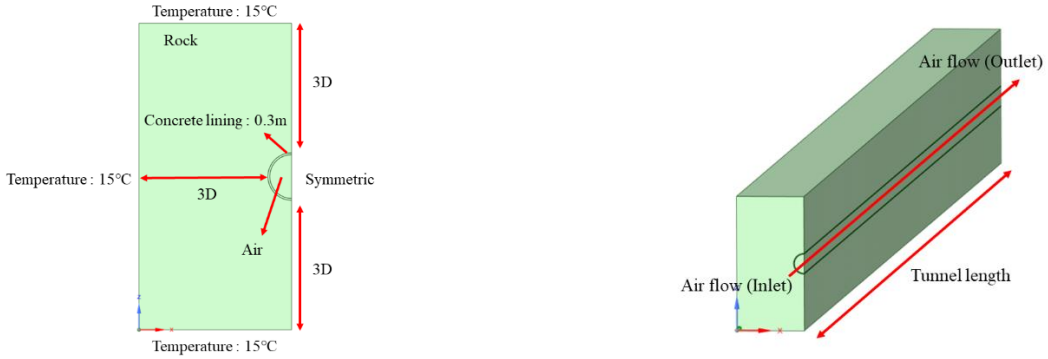

(a) 2D Modeling (b) 3D Modeling

Fig. 4 Tunnel modeling and boundary conditions for model validation

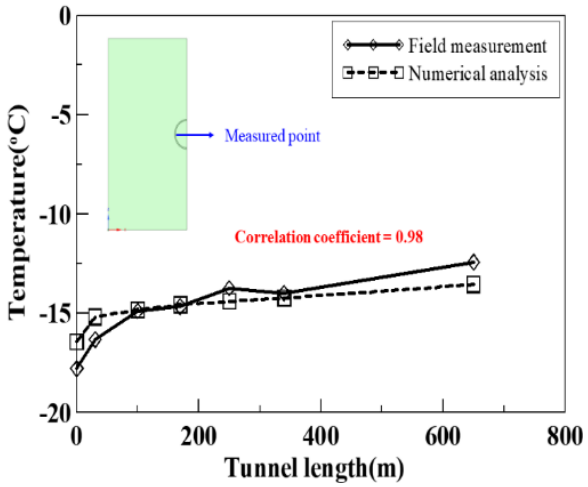

Fig. 5 Results of model validation

the left and upper/lower parts of the rock, and a Symmetric condition was applied to the right boundary of the model. The entrance and exit of the tunnel were set with Inlet and Outlet conditions to allow the inflow and outflow of ambient temperature, with specified wind velocity and temperature conditions. Fig. 3 shows the tunnel modeling for thermal analysis.

3.3 Model validation

Prior to examining the temperature distribution, the numerical analysis model was validated within the tunnel and lining and ground temperature distribution, a comparison and analysis between the field measurement results and the analytical results were conducted. The data from field temperature measurements were obtained from the temperature distribution measurements conducted by Kim *et al*. (2011) in the Hwaak Tunnel. According to the measurement results, the internal temperature distribution of the tunnel showed a trend of the lowest temperature at the tunnel entrance and an increase in temperature towards the exit. The subsurface temperature distribution indicated a consistent temperature of approximately 9°C at a depth of 10 meters regardless of the external temperature. Utilizing the aforementioned field measurement results, the validation of the model was performed by incorporating the field conditions as follows.

Firstly, the Hwaak Tunnel was assumed to have a numerical analysis cross-sectional shape of a circular tunnel with a diameter of 7 m, considering that it has a width of 7.3 m, height of 7 m, and a length of 680 m. Regarding the boundary conditions, the subsurface temperature distribution results of the Hwaak Tunnel were applied.

Table 4 Numerical analysis conditions

Parameter		Value			
Environmental parameter	Air temperature(℃)	-5	-10	-15	-20
	Wind velocity(m/s)	1	2	3	
	Wind direction	One-way	Two-way		
Tunnel Structural Parameter	Tunnel diameter(m)	7	11	15	
	Tunnel length(m)	500	1,000	3,000	5,000

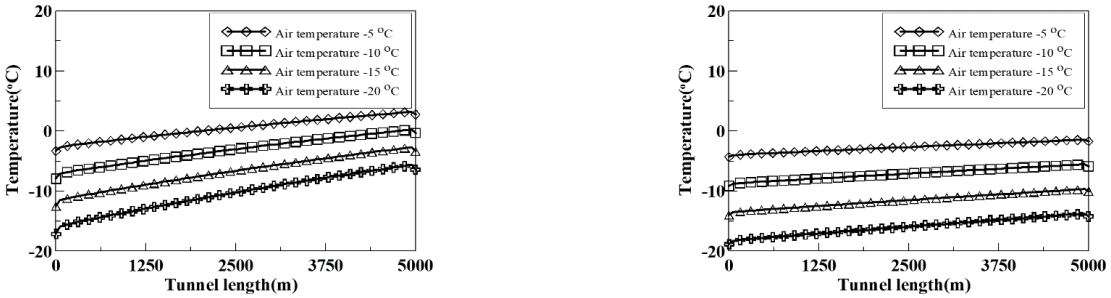

(a) Wind velocity 1 m/s, tunnel length 5,000 m (b) Wind velocity 3 m/s, tunnel length 5,000 m

Fig. 6 Distribution of tunnel internal temperature (tunnel diameter: 11 m, one-way)

A temperature condition of 9℃ was applied to the left side and upper and lower boundaries. Additionally, an external temperature of -18℃ with a wind velocity of 2 m/s was applied at the tunnel entrance, representing the inflow into the tunnel. The temperature measurement points within the numerical analysis were set at the same locations as the field measurements, which are 0 m, 30 m, 100 m, 170 m, 250 m, 340 m, and 650 m from the tunnel entrance, to observe the temperatures along the tunnel sidewalls.

The validation of the model showed an average error of approximately 0.09℃ (4.5%) compared to the field measurements, and a high correlation coefficient of 0.98, indicating a strong correlation. This signifies that the model is effective in performing thermal analysis of the tunnel. Fig. 4 displays the tunnel modeling and boundary conditions for the validation of the model, while Fig. 5 presents the validation results of the model using the field measurement data from the Hwaak Tunnel. Furthermore, Table 3 summarizes the results of the model validation.

3.4 Numerical analysis conditions

The numerical analysis conducted in this study considered the structural and environmental conditions of the tunnel. Parameters related to the structural conditions of the tunnel, such as diameter and length, were taken into account.

Parameters related to the environmental conditions of the tunnel, including external temperature, wind velocity, and wind direction, were also selected.

In consideration of the structural conditions of the tunnel, the tunnel diameter was selected based on the cross-sectional types, including small section, standard section, and large section. For a circular tunnel, diameters of 7 m, 11 m, and 15 m were chosen. According to the investigation and planning guidelines for tunnel design (KDS 27 10 10, 2016), tunnels are categorized as short tunnels for lengths less than 1,000 m, long tunnels for lengths ranging from 1,000 m to 5,000 m, and very long tunnels for lengths exceeding 5,000 m. Therefore, tunnel lengths of 500 m, 1,000 m, 3,000 m, and 5,000 m were selected.

For the environmental conditions of the tunnel, the outdoor temperatures considered were based on meteorological data from Gangwon Province, which is representative of a cold region in South Korea. To account for tunnel designs in even colder regions, temperatures of -5°C, -10°C, -15°C, and -20°C were selected. As for wind velocity, an average wind velocity of 2 m/s in Gangwon Province was taken into account, and wind velocity of 1 m/s, 2 m/s, and 3 m/s were selected. The wind direction was defined as one-way (referred to as "One") when sub-zero temperature air flows into the tunnel entrance and exits at the tunnel exit. It was defined as two-way (referred to as "Two") when sub-zero temperature air flows into both the tunnel entrance and exit. Therefore, two conditions, one-way and two-way, were chosen. In this study, steady-state analysis was conducted, which does not consider changes over time. The temperature measurements were taken at intervals of 50 m along the tunnel walls for the internal tunnel temperature. For the tunnel ground temperature, measurements were taken at intervals of 1 m from the concrete lining wall to the ground at the tunnel entrance (0% of the total length), the middle section of the tunnel (50% of the total length), and the tunnel exit (100% of the total length) when the wind direction was one-way. When the wind direction was two-way, measurements were taken at intervals of 1 m from the concrete lining wall to the ground at the tunnel entrance (0% of the total length), between the entrance and middle section (25% of the total length), and the middle section of the tunnel (50% of the total length). Table 4 presents the numerical analysis conditions considered in this study.

4. Results of numerical analysis

4.1 Temperature distribution according to wind velocity when wind direction is one-way

4.1.1 Internal temperature

When cold air enters the tunnel only from the entrance direction (one-way) and is below freezing, the internal temperature distribution of the tunnel was found to be lowest at the tunnel entrance and gradually increased towards the tunnel exit, followed by a decrease. In the case of shorter tunnels (500 m), the entire tunnel section maintained a sub-zero temperature distribution under all external temperature conditions, and it was confirmed that the entire tunnel section exhibited a freezing-susceptible temperature distribution below -7℃ when the external temperature dropped below -10℃. However, as the tunnel length increased, there was an increase in the sections maintaining temperatures above freezing and sections maintaining temperatures above -7℃.

In the case of a tunnel with a diameter of 11 m, the temperature distribution within a 500 m long tunnel showed an average temperature decrease of 1.06℃ when the wind velocity increased from 1 m/s to 2 m/s and an average temperature decrease of 0.42℃ when the wind velocity increased from 2 m/s to 3 m/s, with an external temperature of -5℃. Additionally, with an external temperature of 10℃, there were temperature decreases of 1.32℃ and 0.53℃, with an external temperature of -15℃, there were temperature of -20℃, there were temperature decreases of 1.85℃ and 0.74℃, respectively. In the case of a 5,000 m long tunnel, with an external temperature of -5℃, there was an average temperature decrease of 2.24℃ and 0.92℃ with increasing wind velocity, and as the external temperature decreased, the temperature decrease gradually decreased, reaching 3.92℃ and 1.61℃ at an external temperature of –20℃.

Therefore, it was observed that the internal temperature distribution of the tunnel decreased with increasing wind velocity, and as the external temperature decreased, the temperature decreases due to wind velocity increased. Additionally, as the tunnel length increased, the temperature decreases grew as wind velocity increasing. Fig. 6 depicts the internal temperature distribution of the tunnel according to increasing wind velocity for various external temperatures when the wind direction is one-way.

4.1.2 Ground temperature

When cold air enters one-way, the temperature distribution in the tunnel ground showed an increasing trend towards the subsurface temperature as the depth from the concrete lining surface to the ground increased. As the depth of the ground increased, the temperature difference between the ground and the outside air decreased. The ground temperature at the entrance (0%), midpoint (50%), and exit (100%) decreased with increasing wind velocity, and the depth maintaining temperatures below 0℃ increased.

When the tunnel has a diameter of 11m and a length of 500 m, at an outside air temperature of -5℃, an increase in wind velocity from 1m/s to 2m/s resulted in an average temperature decrease of 0.35℃ at the tunnel entrance (0%), 0.41℃ at the midpoint (50%), and 0.44℃ at the tunnel exit (100%). Similarly, when the wind velocity increased from 2m/s to 3m/s, there was an average temperature decrease of 0.14℃ at the tunnel entrance (0%), 0.16℃ at the midpoint (50%), and 0.18℃ at the tunnel exit (100%). At an outside air temperature of -10℃, an increase in wind velocity led to temperature decreases of 0.43℃ and 0.17℃ at the tunnel entrance, 0.51℃ and 0.2℃ at the midpoint, and 0.55℃ and 0.22℃ at the tunnel exit. For an outside air temperature of 15℃, the corresponding temperature decreases were 0.52℃ and 0.2℃ at the tunnel entrance, 0.62℃ and 0.24℃ at the midpoint, and 0.66℃ and 0.26℃ at the tunnel exit as the wind velocity increased. At an outside air temperature of -20℃, as the wind velocity increased, the temperature decreases were 0.60℃ and 0.24℃ at the tunnel entrance, 0.72℃ and 0.29℃ at the midpoint, and 0.77℃ and 0.31℃ at the tunnel exit.

For an extremely long tunnel with a length of 5,000m, at an outside air temperature of -5℃, the temperature decrease at the tunnel entrance was 0.35℃ and 0.14℃, at the midpoint it was 0.8℃ and 0.32℃, and at the tunnel exit it was 1.1℃ and 0.47℃, respectively. Furthermore, at an outside air temperature of -20℃, the temperature decrease at the tunnel entrance was an average of 0.61℃ and 0.24℃, at the midpoint it was 1.4℃ and 0.57℃, and at the tunnel exit it was 1.93℃ and 0.82℃. Fig. 7 presents a graph showing the temperature distribution of the ground with respect to the increase in wind velocity when the wind direction is one-way.

4.2 Temperature distribution according to wind velocity when wind direction is two-way

4.2.1 Internal temperature

When air with below-freezing temperatures flows into the tunnel from both the entrance and exit directions(two-way), the temperature distribution inside the tunnel exhibits a symmetric pattern, with the lowest temperatures observed at the entrance and exit regions and gradually increasing towards the center of the tunnel. For a tunnel length of 500 m, at a wind velocity of 1 m/s and an outside temperature of -5℃, certain sections in the central part of the tunnel maintain temperatures above freezing, and if the wind velocity exceeds 2 m/s and the outside temperature is below -10℃, the entire tunnel experiences sub-freezing temperatures. As the tunnel length increases, there are more sections that either maintain temperatures above freezing or exhibit unfrozen regions with temperatures above -7℃. In the case of very long tunnel (5,000 m), there are regions in the central part where the temperature remains above 10℃.

For a tunnel with a diameter of 11 m, in the case of a 500 m tunnel length and an outside temperature of -5℃, as the wind velocity increases from 1 m/s to 2 m/s and from 2 m/s to 3 m/s, the average temperature inside the tunnel decreases y approximately 1.35℃ and 0.56℃, respectively. When the outside temperature is -10℃, the temperature inside the tunnel decreases by approximately 1.68℃ and 0.7℃ as the wind velocity increases. Similarly, for an outside temperature of -15℃, the temperature decreases by

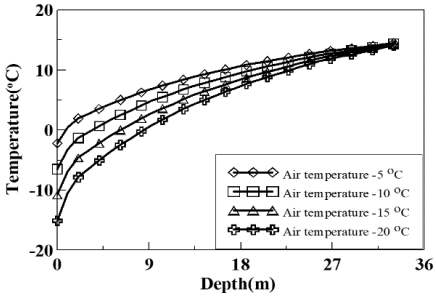

(a) Wind velocity 1 m/s, tunnel length 5,000 m, 0% point

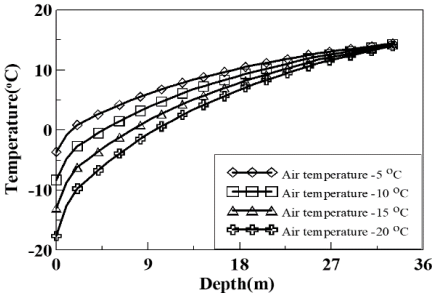

(b) Wind velocity 3 m/s, tunnel length 5,000 m, 0% point

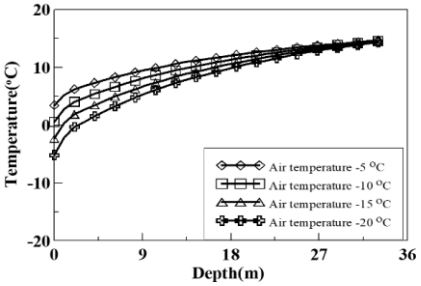

(c) Wind velocity 1 m/s, tunnel length 5,000 m, 100% point

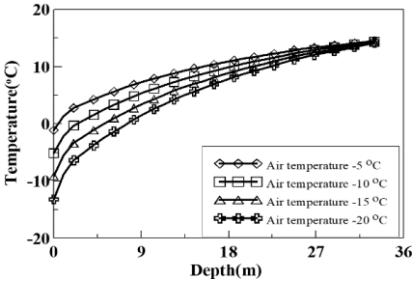

(d) Wind velocity 3 m/s, tunnel length 5,000 m, 100% point

Fig. 7 Distribution of tunnel ground temperature (tunnel diameter: 11 m, one-way)

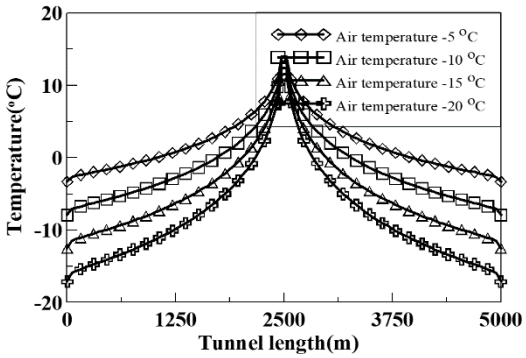

(a) Wind velocity 1 m/s, tunnel length 5,000 m

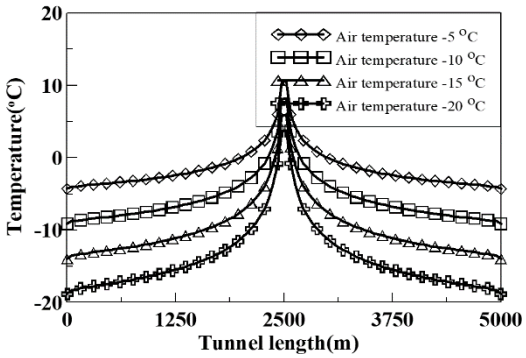

(b) Wind velocity 3 m/s, tunnel length 5,000 m

Fig. 8 Distribution of tunnel internal temperature (tunnel diameter: 11 m, two-way)

approximately 2.02℃ and 0.84℃, and for an outside temperature of -20℃, the temperature decreases by approximately 2.37℃ and 0.98℃. For a tunnel length of 1,000 m, at an outside temperature of -5℃, the average temperature inside the tunnel decreases by approximately 1.64℃ and 0.7℃, and at an outside temperature of -20℃, the temperature decreases by approximately 2.87℃ and 1.23℃. In the case of an very long tunnel with a length of 5,000 m, at an outside temperature of -5℃, the average temperature inside the tunnel decreases by approximately 2.23℃ and 1.04℃, and at an outside temperature of -20℃, the temperature decreases by approximately 3.93℃ and 1.83℃.

Even when the wind direction is two-way, the temperature distribution inside the tunnel showed a decreasing trend as the wind velocity increased, similar to the case of one-way airflow. It was also observed that as the outside temperature decreased, the temperature decreases due to wind velocity also increased. Furthermore, as the tunnel length increased and the wind velocity increased, the magnitude of temperature decreases also increased. Fig. 8 displays the graph showing the distribution of internal temperatures in the tunnel according to the increase in wind velocity for two-way airflow.

4.2.2 Ground temperature

When cold air flows in two-way, the temperature distribution of the tunnel's ground showed a similar trend to that of one-way airflow, where the temperature gradually increased towards the subsurface temperature as the depth from the lining surface to the ground increased. In the case of a short tunnel with a length of 500 m, the temperature distribution of the ground at the tunnel's center (50%) exhibited a zone where the surface temperature of the lining remained below freezing, regardless of changes in wind velocity and outside temperature. However, for a tunnel with a length of 1,000 m, the temperature distribution of the ground at the tunnel's center showed that the lining surface temperature maintained freezing temperatures when the ind velocity was 1 m/s and the outside temperature was -5℃ or -10℃. For a tunnel with a length of 5,000 m, the temperature distribution of the ground at the tunnel's center

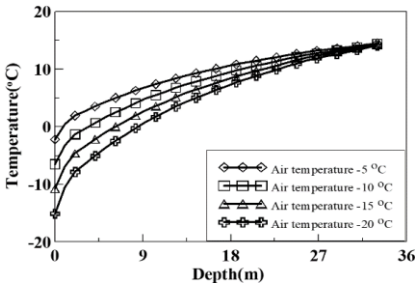

(a) Wind velocity 1 m/s, tunnel length 5,000 m, 0% point

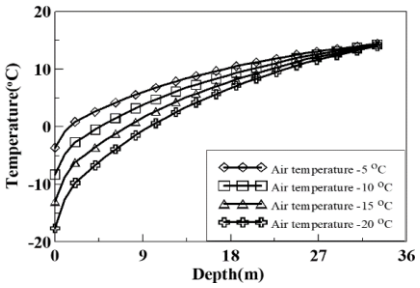

(b) Wind velocity 3 m/s, tunnel length 5,000 m, 0% point

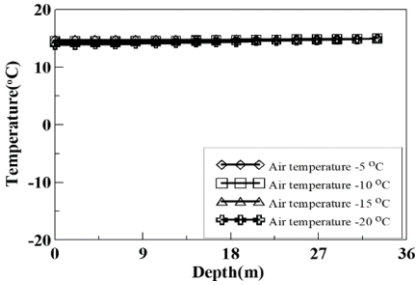

(c) Wind velocity 1 m/s, tunnel length 5,000 m, 50% point

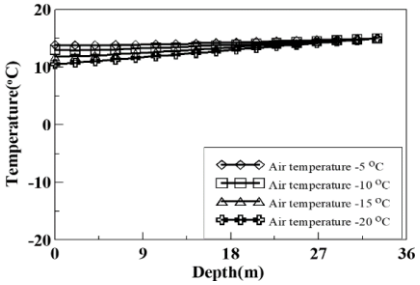

(d) Wind velocity 3 m/s, tunnel length 5,000 m, 50% point

Fig. 9 Distribution of tunnel ground temperature (tunnel diameter: 11 m, two-way)

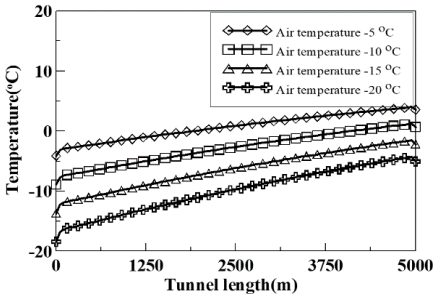

(a) Wind velocity 1 m/s, tunnel length 5,000 m

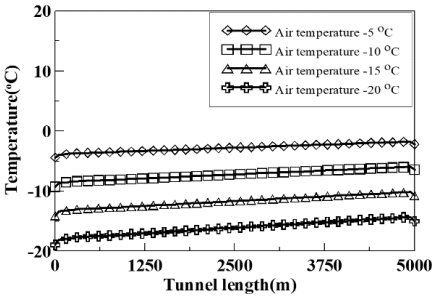

(b) Diameter 15 m, tunnel length 5,000 m

Fig. 10 Distribution of tunnel internal temperature (wind velocity: 2m/s, one-way)

consistently maintained temperatures above 10℃, regardless f wind velocity and outside temperature.

When quantitatively analyzing the temperature distribution of the surrounding ground surface with increasing wind velocity and varying outdoor temperatures, in the case of a tunnel with a diameter of 11 m and a length of 500 m, at an outdoor temperature of -5℃, the temperature at the tunnel entrance (0%) decreased by an average of 0.35℃, 0.14℃ as the wind velocity increased. At the section between the tunnel entrance and the middle (25%), the temperature decreased by 0.53℃, 0.22℃, and at the tunnel's middle section, it decreased by 0.58℃, 0.24℃. For an outdoor temperature of -10℃, at the tunnel entrance and the section between the entrance and middle, the temperature decrease at the tunnel's middle section increased with increasing wind velocity, showing decreases of 0.44℃, 0.17℃, 0.66℃, 0.27℃, 0.73℃, and 0.3℃, respectively. At an outdoor temperature of -15℃, the temperature decrease at the tunnel entrance and the section between the entrance and middle also increased with increasing wind velocity. At the tunnel's middle section, the temperature decreases were 0.52℃, 0.21℃, 0.8℃, 0.33℃, 0.87℃, and 0.35℃, respectively. Furthermore, at an outdoor temperature of -20℃, the temperature decreases were 0.62℃, 0.24℃, 0.94℃, 0.38℃, 1.02℃, and 0.41℃.

For an extremely long tunnel with a length of 5,000 m, at an outdoor temperature of -5℃, it was observed that the temperature decreases with differences of 0.35℃, 0.14℃, 0.78℃, 0.33℃, 0.3℃, and 0.25℃, respectively. At an outdoor temperature of -20℃, the average temperature decreases were 0.61℃, 0.24℃, 1.37℃, 0.58℃, 0.92℃, and 0.7℃. Fig. 9 displays the temperature distribution of the surrounding ground surface with increasing wind velocity at arious outdoor temperatures when the wind direction is two-way.

4.3.2 Ground temperature

When air with subzero temperatures flows one-way, it was observed that the temperature distribution of the tunnel surrounding ground decreases at the entrance (0%), middle section (50%), and exit (100%) as the tunnel diameter increases. Additionally, the depth maintaining temperatures below 0°C increases. Furthermore, at a wind velocity of 2 m/s, for a tunnel with a diameter of 7 m and a length of 5,000 m, it was observed that the middle section maintains temperatures similar to the surface of the concrete lining when the outside temperature was -5°C, while at the exit, temperatures similar to the surface of the concrete lining

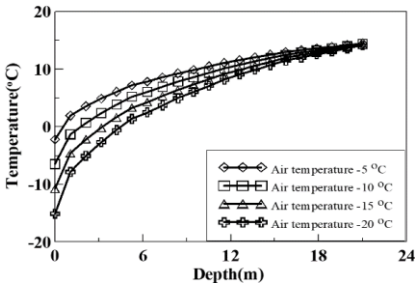

(a) Diameter 7 m, tunnel length 5,000 m, 0% point

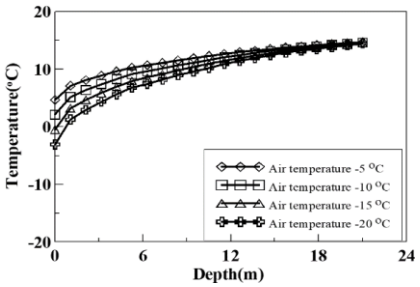

(b) Diameter 7 m, tunnel length 5,000 m, 100% point

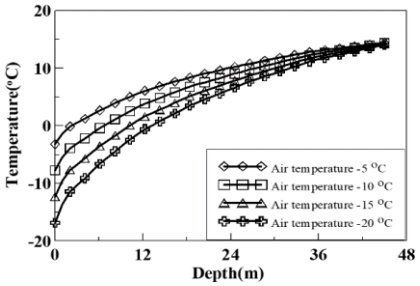

(c) Diameter 15 m, tunnel length 5,000 m, 0% point

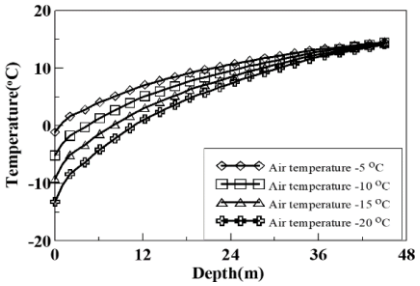

(d) Diameter 15 m, tunnel length 5,000 m, 100% point

Fig. 11 Distribution of tunnel ground temperature (wind velocity: 2m/s, one-way)

were maintained when the outside temperature was -5°C and -10°C.

At a wind velocity of 2 m/s, for a tunnel with a length of 500 m and an outside temperature of -5°C, it was observed that increasing the tunnel diameter from 7 m to 11 m resulted in an average temperature decrease of 2.82°C at the tunnel entrance, and increasing it from 11 m to 15 m resulted in a decrease of 1.73°C. Similarly, at the tunnel's middle section, as the tunnel diameter increased, temperature decreases of 2.95°C and 1.82°C were observed, while at the tunnel exit, temperature decreases of 2.91°C and 1.78°C were observed. When the outside temperature was -10°C, increasing the tunnel diameter resulted in average temperature decreases of 3.52°C and 2.16°C at the entrance, 3.68°C and 2.28°C at the middle section, and 3.64°C and 2.22°C at the exit. At an outside temperature of -15°C, average temperature decreases of 4.23°C and 2.59°C were observed at the entrance, 4.42°C and 2.73°C at the middle section, and 4.37°C and 2.67°C at the exit. When the outside temperature was -20°C, increasing the tunnel diameter led to temperature decreases of 4.93°C and 3.02°C at the entrance, 5.16°C and 3.19°C at the middle section, and 5.09°C and 3.11°C at the exit. For a tunnel with a length of 5,000 m, when the outside temperature was -5°C, increasing the tunnel diameter resulted in temperature decreases of 3.21°C and 1.77°C at the entrance, 3.7°C and 2.07°C at the middle section, and 3.75°C and 2.25°C at the exit. Similarly, at an outside temperature of -20°C, increasing the tunnel diameter led to temperature decreases of 5.62°C and 3.11°C at the entrance, 6.47°C and 3.62°C at the middle section, and 6.56°C and 3.94°C at the exit. Fig. 11 depicts the temperature distribution of the tunnel surrounding ground with increasing tunnel diameter at different outside temperatures when the wind direction is one-way.

4.3 Temperature distribution according to tunnel diameter when wind direction is one-way

4.3.1 Internal temperature

When the wind direction is one-way, the internal temperature distribution according to tunnel diameter follows the same pattern as the temperature distribution within the tunnel based on wind velocity.

When considering the internal temperature distribution in the tunnel at a wind velocity of 2 m/s, for a tunnel with a length of 500 m and an outside temperature of -5℃, an increase in tunnel diameter from 7 m to 11 m resulted in an average temperature decrease of 0.69℃, while an increase from 11 m to 15 m resulted in an average temperature decrease of 0.36℃. At an outside temperature of -10℃, an increase in tunnel diameter from 7 m to 11 m led to an average temperature decrease of 0.87℃, and an increase from 11 m to 15 m resulted in an average temperature decrease of 0.45℃. For an outside temperature of -15℃, with a tunnel diameter increase from 7 m to 11 m and from 11 m to 15 m, there was an average temperature decrease of 1.04℃ and 0.55℃, respectively. At an outside temperature of -20℃, there were temperature decreases of 1.21℃ and 0.64℃, respectively. In the case of very long tunnel with a length of 5,000 m and an outside temperature of -5℃, an increase in tunnel diameter resulted in temperature decreases of 2.48℃ and 1.03℃, while at an outside temperature of -20℃, there were temperature decreases of 4.35℃ and 1.79℃, respectively.

Therefore, as the tunnel diameter increased, the internal tunnel temperature decreases, and it was observed that the temperature decrease becomes greater as the outside temperature decreases. Additionally, as the length of the tunnel increases, the temperature decrease also increases with the increase in tunnel diameter. Fig. 10 displays the

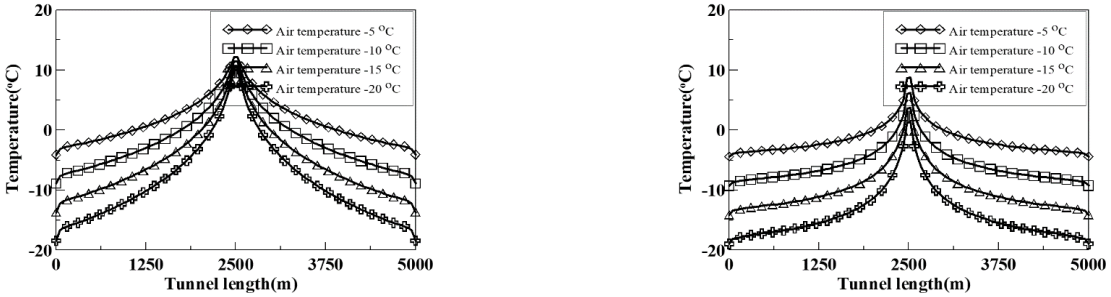

(a) Diameter 7 m, tunnel length 5,000 m (b) Diameter 15 m, tunnel length 5,000 m

Fig. 12 Distribution of tunnel internal temperature (wind velocity: 2m/s, two-way)

distribution of internal tunnel temperature with respect to outside temperature for a one-way wind flow, as the tunnel diameter increases.

4.3.2 Ground temperature

When air with subzero temperatures flows one-way, it was observed that the temperature distribution of the tunnel surrounding ground decreases at the entrance (0%), middle section (50%), and exit (100%) as the tunnel diameter increases. Additionally, the depth maintaining temperatures below 0°C increases. Furthermore, at a wind velocity of 2 m/s, for a tunnel with a diameter of 7 m and a length of 5,000 m, it was observed that the middle section maintains temperatures similar to the surface of the concrete lining when the outside temperature was -5°C, while at the exit, temperatures similar to the surface of the concrete lining were maintained when the outside temperature was -5°C and -10°C.

At a wind velocity of 2 m/s, for a tunnel with a length of 500 m and an outside temperature of -5°C, it was observed that increasing the tunnel diameter from 7 m to 11 m resulted in an average temperature decrease of 2.82°C at the tunnel entrance, and increasing it from 11 m to 15 m resulted in a decrease of 1.73°C. Similarly, at the tunnel's middle section, as the tunnel diameter increased, temperature decreases of 2.95°C and 1.82°C were observed, while at the tunnel exit, temperature decreases of 2.91°C and 1.78°C were observed. When the outside temperature was -10°C, increasing the tunnel diameter resulted in average temperature decreases of 3.52°C and 2.16°C at the entrance, 3.68°C and 2.28°C at the middle section, and 3.64°C and 2.22°C at the exit. At an outside temperature of -15°C, average temperature decreases of 4.23°C and 2.59°C were observed at the entrance, 4.42°C and 2.73°C at the middle section, and 4.37°C and 2.67°C at the exit. When the outside temperature was -20°C, increasing the tunnel diameter led to temperature decreases of 4.93°C and 3.02°C at the entrance, 5.16°C and 3.19°C at the middle section, and 5.09°C and 3.11°C at the exit. For a tunnel with a length of 5,000 m, when the outside temperature was -5°C, increasing the tunnel diameter resulted in temperature decreases of 3.21°C and 1.77°C at the entrance, 3.7°C and 2.07°C at the middle section, and 3.75°C and 2.25°C at the exit. Similarly, at an outside temperature of -20°C, increasing the tunnel diameter led to temperature decreases of 5.62°C and 3.11°C at the entrance, 6.47°C and 3.62°C at the middle section, and 6.56°C and 3.94°C at the exit. Fig. 11 depicts the temperature distribution of the tunnel surrounding ground with increasing tunnel diameter at different outside temperatures when the wind direction is one-way.

4.4 Temperature distribution according to tunnel diameter when wind direction is two-way

4.4.1 Internal temperature

When the wind direction is two-way, the distribution of internal temperature in relation to the tunnel diameter exhibited a symmetrical trend with the highest temperature occurring at the central portion, excluding a 15 m diameter, 500 m long tunnel. The temperature difference was smallest at the entrance and exit of the tunnel, while it was largest at the center of the tunnel.

For the case of tunnel internal temperature distribution at a wind velocity of 2 m/s, considering a 500 m short tunnel with an outside temperature of -5°C, increasing the tunnel diameter from 7 m to 11 m resulted in an average temperature decrease of 0.88°C, while increasing the diameter from 11 m to 15 m led to an average temperature decrease of 0.39°C. When the outside temperature was -10°C, increasing the tunnel diameter from 7 m to 11 m resulted in an average temperature decrease of 1.1°C, and increasing the diameter from 11 m to 15 m led to an average temperature decrease of 0.49°C. With an outside temperature of -15°C, increasing the tunnel diameter from 7 m to 11 m resulted in an average temperature decrease of 1.32°C, and increasing the diameter from 11m to 15m led to an average temperature decrease of 0.59°C. With an outside temperature of -20°C, the temperature decreases were 1.54°C and 0.69°C, respectively.

In the case of a very long tunnel of 5,000 meters, with an outside temperature of -5°C, increasing the tunnel diameter showed temperature decreases of 1.99°C and 1.11°C, while at an outside temperature of -20°C, the temperature decreases were 3.55°C and 1.93°C, respectively. Fig. 12 displays the distribution of internal temperatures in the tunnel with varying tunnel diameters according to outside temperature, in the case of two-way wind direction.

4.4.2 Ground temperature

When cold air flows two-way, it was observed that as

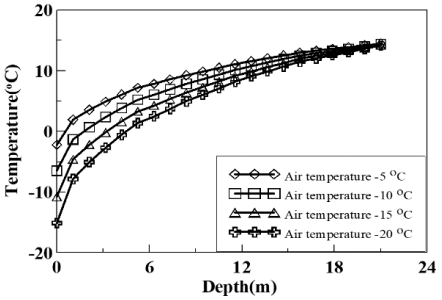

(a) Diameter 7 m, tunnel length 5,000 m, 0% point

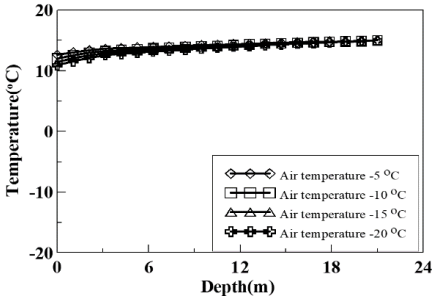

(b) Diameter 7 m, tunnel length 5,000 m, 50% point

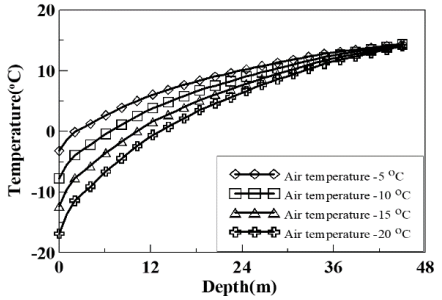

(c) Diameter 15 m, tunnel length 5,000 m, 0% point

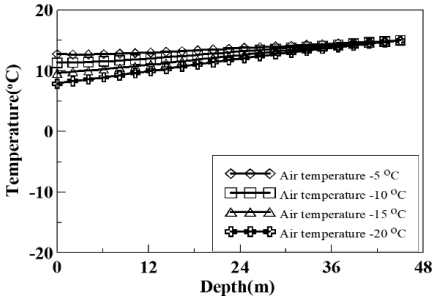

(d) Diameter 15 m, tunnel length 5,000 m, 50% point

Fig. 13 Distribution of tunnel ground temperature (wind velocity: 2 m/s, two-way)

the tunnel diameter increased, the temperature distribution of the tunnel's surrounding ground exhibited a similar trend to the temperature distribution of the surrounding ground based on wind velocity.

Quantitative analysis of the temperature distribution of the surrounding ground depending on the tunnel diameter revealed that for a tunnel length of 500 m and an outside temperature of -5°C, increasing the tunnel diameter from 7 m to 11 m resulted in an average temperature decrease of 2.82°C at the tunnel entrance, and increasing the diameter from 11 m to 15 m led to a decrease of 1.73°C. Between the tunnel entrance and the center, as the tunnel diameter increased, there were temperature decreases of 2.98°C and 1.85°C, respectively, and at the tunnel center, decreases of 3.67°C and 1.84°C, respectively. At an outside temperature of -10°C, increasing the tunnel diameter resulted in average temperature decreases of 3.52°C and 2.16°C at the entrance, 3.73°C and 2.32°C between the entrance and the center, and 4.58°C and 2.29°C at the center. When the outside temperature was -15°C, there were average temperature decreases of 4.23°C and 2.59°C at the entrance, 4.47°C and 2.78°C between the entrance and the center, and 5.5°C and 2.75°C at the center. At an outside temperature of -20°C, increasing the tunnel diameter resulted in temperature decreases of 4.93°C and 3.02°C at the entrance, 5.22°C and 3.24°C between the entrance and the center, and 6.41°C and 3.21°C at the exit. For a very long tunnel with a length of 5,000m, at an outside temperature of -5°C, increasing the tunnel diameter resulted in temperature decreases of 3.21°C and 1.77°C at the entrance, 3.49°C and 1.99°C between the entrance and the center, and 0.17°C and 1.38°C at the center. When the outside temperature was -20°C, increasing the tunnel diameter led to temperature decreases of 5.62°C and 3.1°C at the entrance, 6.11°C and 3.49°C between the entrance and the center, and 0.7°C and 3.24°C at the center.

Fig. 13 depicts the temperature distribution of the surrounding ground with increasing tunnel diameter for two-way directions of wind. It shows the temperature distribution of the ground with respect to outside temperature.

5. Freezing range of a tunnel

5.1 Determination of freezing range by variable

The freezing range of the tunnel was determined by utilizing the numerical analysis results considering the structural and environmental conditions. Regression analysis was conducted for each analysis condition to determine the freezing positions of the tunnel interior and the surrounding ground. The internal temperature of the tunnel was determined by identifying the segment where the temperature remains below -7°C for 2-3 consecutive days, taking into account the occurrence of tunnel freezing damage mentioned in the Korea Expressway Corporation (2013) guidelines. The temperature range where the surrounding ground remains below 0°C was determined.

For the freezing positions according to the internal temperature of the tunnel, the calculated freezing positions for each condition were normalized based on the tunnel length using the freezing rate, as normalized in Eq. (4).

$$F_R(\%) = \frac{F_L(m)}{L(m)} \times 100 \quad (4)$$

Where F_R is the freezing rate, F_L is the freezing length, L is the tunnel length.

5.1.1 Freezing rate and freezing depth according to outside air temperature

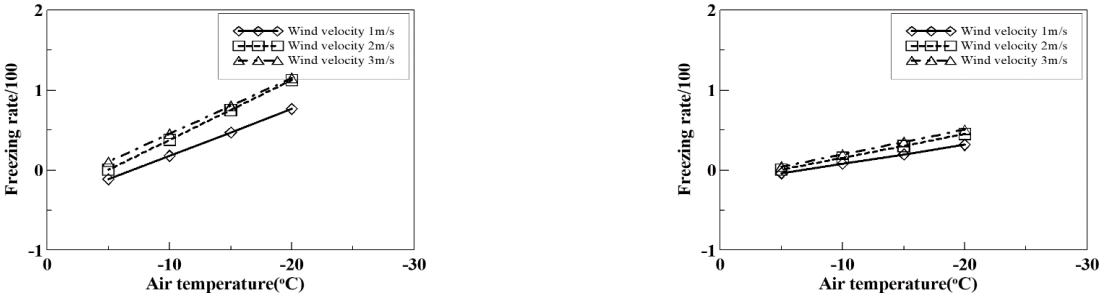

(a) One-way (b) Two-way

Fig. 14 Freezing rate according to the air temperature

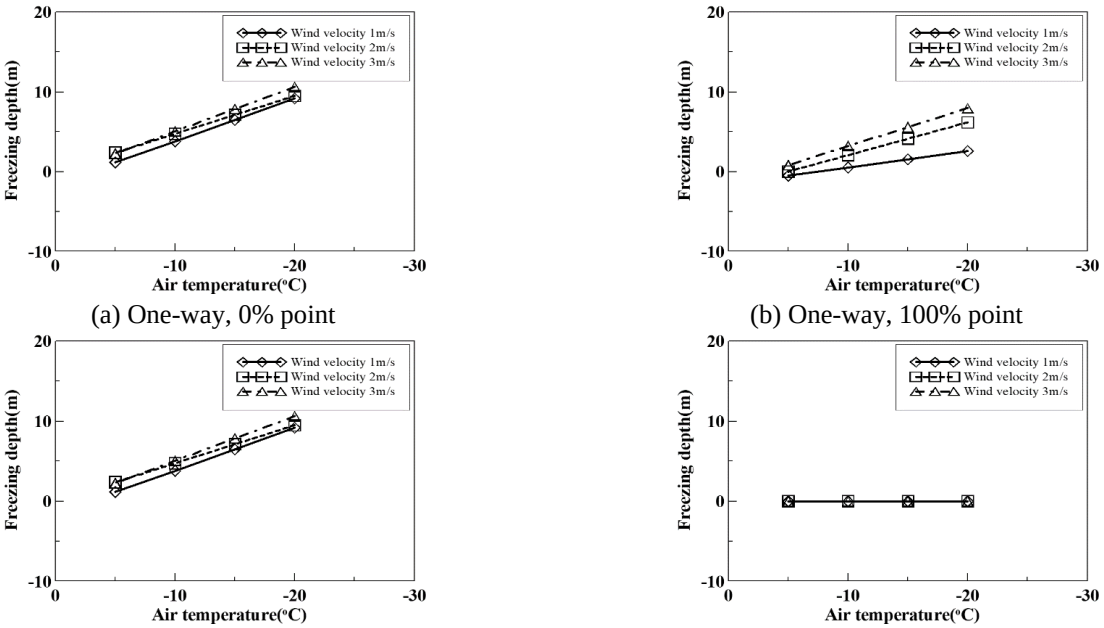

(a) One-way, 0% point (b) One-way, 100% point

(c) Two-way, 0% point (d) Two-way, 50% point

Fig. 15 Freezing depth according to the air temperature

(1) Internal temperature

The freezing rate of the tunnel varied with the outside air temperature when air with sub-zero temperatures flowed into the tunnel in a one-way or two-way manner. It showed an increasing trend as the outside air temperature decreased, although the rate of increase in the freezing rate was relatively lower for two-way flow compared to one-way flow. This can be attributed to the fact that in one-way flow, the internal temperature of the tunnel gradually increased towards the exit, with the highest temperature observed just before the exit. In contrast, in two-way flow, the highest temperature was observed at the central section of the tunnel.

For example, in a one-way tunnel with a diameter of 11 m and a length of 5,000 m, at a wind velocity of 1m/s, a decrease in outside air temperature from -5°C to -10°C resulted in a 2% increase in the freezing rate. Similarly, a decrease from -10°C to -15°C led to a 43% increase in the freezing rate, and a decrease from -15°C to -20°C resulted in a 37% increase. Under the same conditions but with a wind velocity of 2m/s, a decrease from -5°C to -10°C resulted in a 26% increase in the freezing rate, a decrease from -10°C to -15°C resulted in a 74% increase, and at -20°C, the freezing rate reached 100%, indicating that the entire tunnel remained below -7°C.

At a wind velocity of 3 m/s, a decrease from -5°C to -10°C resulted in a 52% increase in the freezing rate, a decrease from -10°C to -15°C resulted in a 48% increase, and at -20°C, the freezing rate reached 100%, indicating the entire tunnel maintained a temperature below -7°C.

In the case of a two-way tunnel, at a wind velocity of 1m/s, a decrease from -5°C to -10°C resulted in a 1% increase in the freezing rate, a decrease from -10°C to -15°C resulted in a 21% increase, and a decrease from -15°C to -20°C resulted in a 10% increase. At a wind velocity of 2m/s, the freezing rate increased by 14%, 21%, and 7% respectively, as the outside air temperature decreased. Similarly, at a wind velocity of 3m/s, the freezing rate increased by 23%, 18%, and 4% respectively, as the outside air temperature decreased. Fig. 14 displays freezing rate according to the air temperature.

(2) Ground temperature

When air with sub-zero temperatures flowed into the tunnel in a one-way or two-way manner, the freezing depth of the surrounding ground showed an increasing trend as

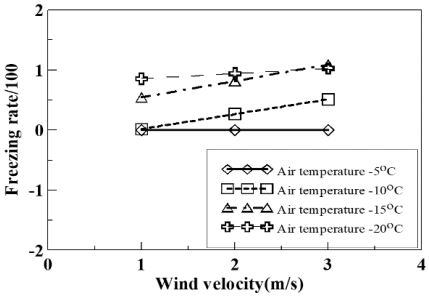

(a) One-way

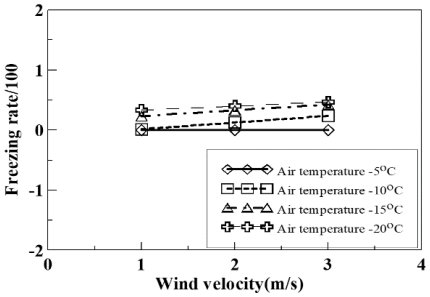

(b) Two-way

Fig. 16 Freezing rate according to the wind velocity

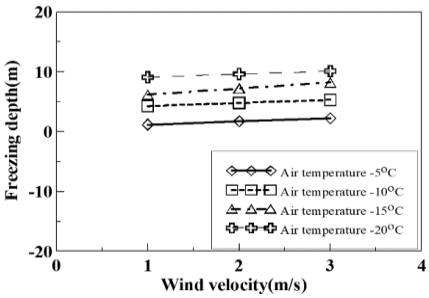

(a) One-way, 0% point

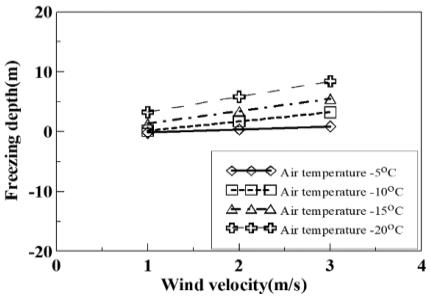

(b) One-way, 100% point

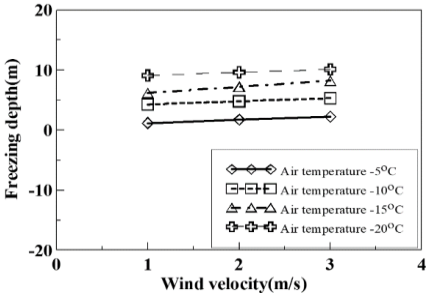

(c) Two-way, 0% point

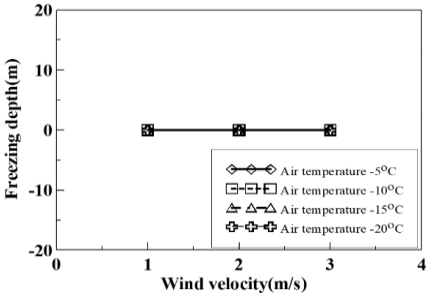

(d) Two-way, 50% point

Fig. 17 Freezing depth according to the wind velocity

the outside air temperature decreased, except for the central section in the case of two-way flow. In the central section of two-way flow, it was determined that the ground maintained a temperature similar to that of the tunnel interior.

For instance, in a one-way tunnel with a diameter of 11 m and a length of 5,000 m, at a wind velocity of 1m/s, a decrease in outside air temperature from -5°C to -10°C resulted in an increase in freezing depth of 3.1m at the tunnel entrance, 2.1 m in the central section, and no increase at the tunnel exit. A decrease from -10°C to -15°C resulted in an increase of 2.1 m in freezing depth at the tunnel entrance and central section, and 1m at the tunnel exit. Similarly, a decrease from -15°C to -20°C resulted in an increase of 3.1 m in freezing depth at the tunnel entrance and 2.1 m in the central section and exit. Under the same conditions but with a wind velocity of 2m/s, a decrease from -5°C to -10°C resulted in an increase of 3.1 m, 3.1 m, and 2.1 m in freezing depth at the entrance, central section, and exit, respectively. A decrease from -10°C to -15°C resulted in an increase of 2.1 m, 2.1 m, and 1 m at the entrance, central section, and exit, respectively. Furthermore, a decrease from -15°C to -20°C resulted in an increase of 2.1 m in freezing depth at all sections: entrance, central, and exit. In the case of a wind velocity of 3 m/s, a decrease from -5°C to -10°C resulted in an increase of 3.1 m, 2.1 m, and 2.1 m in freezing depth at the entrance, central section, and exit, respectively. A decrease from -10°C to -15°C resulted in an increase of 3.1 m, 3.1 m, and 2.1 m at the entrance, central section, and exit, respectively. At -20°C, the freezing depth increased by 2.1 m, 2.1 m, and 3.1 m at the entrance, central section, and exit, respectively. Fig. 15 displays Freezing depth according to the air temperature.

5.1.2 Freezing rate and freezing depth according to wind velocity

(1) Tunnel Interior Temperature

When air with sub-zero temperatures flowed into the tunnel in a one-way or two-way manner, the freezing rate of the tunnel showed an increasing trend as the wind velocity increased, except when the external air temperature was -5°C. This can be attributed to the fact that there was no section in the tunnel where the interior temperature remained below -7°C when the outside air temperature was -5°C.

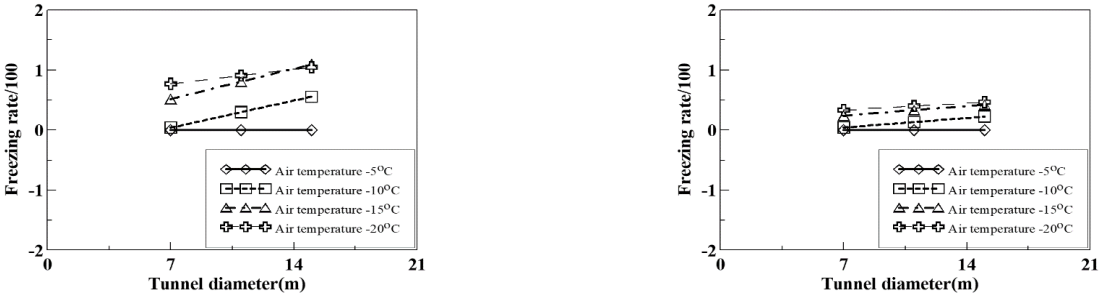

(a) One-way (b) Two-way

Fig. 18 Freezing rate according to the diameter

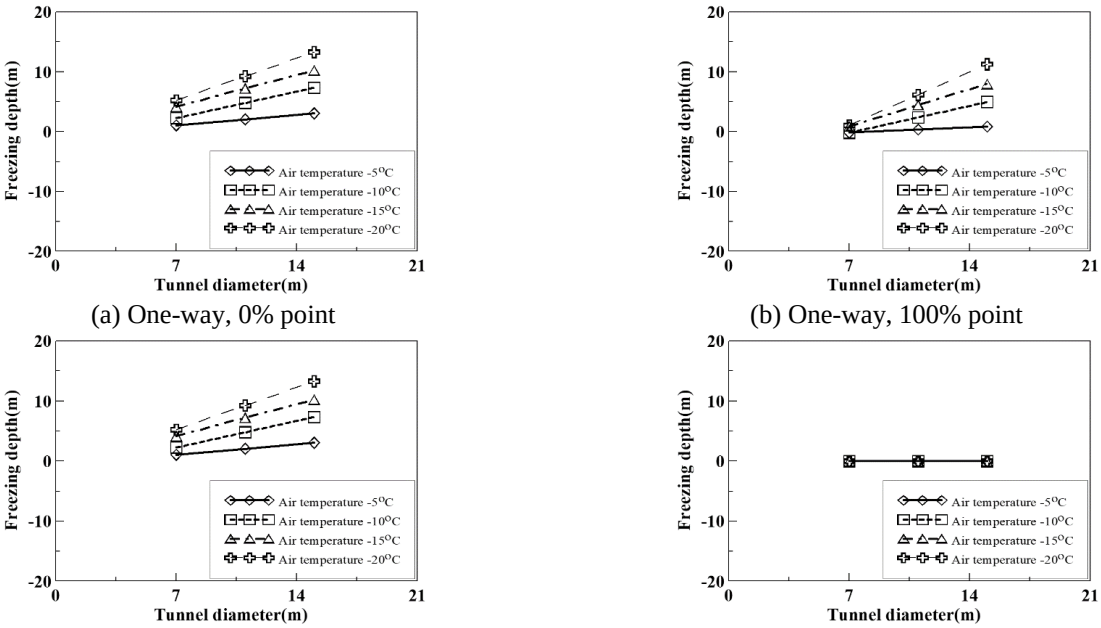

(a) One-way, 0% point (b) One-way, 100% point

(c) Two-way, 0% point (d) Two-way, 50% point

Fig. 19 Freezing depth according to the diameter

In the case of one-way flow with a tunnel diameter of 11 m and a length of 5,000 m, at an outside air temperature of -5°C, the freezing rate remained at 0% regardless of the wind velocity. At an outside air temperature of -10°C, the freezing rate increased by 24% and 25% as the wind velocity increased. Furthermore, at an outside air temperature of –15°C, the freezing rate increased by 55% as the wind velocity increased from 1 m/s to 2 m/s, and the freezing rate reached 100% at wind velocity of 2 m/s and 3 m/s. At an outside air temperature of -20°C, the freezing rate increased by 17% as the wind velocity increased from 1 m/s to 2 m/s, and the freezing rate remained at 100% at wind velocity of 2 m/s and 3 m/s. In the case of two-way flow, the freezing rate remained at 0% as the wind velocity increased when the outside air temperature was -5°C, similar to the one-way flow. At an outside air temperature of -10°C, the freezing rate increased by 13% and 9% as the wind velocity increased. When the outside air temperature was -15°C, the freezing rate increased by 13% and 6% as the wind velocity increased. Additionally, at an outside air temperature of -20°C, the freezing rate increased by 10% and 3%, respectively. Fig. 16 displays freezing rate according to the wind velocity.

(2) Tunnel Ground

When air with sub-zero temperatures flowed into the tunnel in a one-way or two-way manner, the freezing depth of the ground showed an increasing trend as the wind velocity increased.

In the case of one-way flow with a tunnel diameter of 11m and a length of 5,000 m, at an outside air temperature of -5°C, the freezing depth increased by 1m at the entrance and remained at 0m at the center, while at the exit, the ground maintained a temperature above freezing until the wind velocity increased to 3 m/s, resulting in a 1m increase in freezing depth. At an outside air temperature of -10°C, at the tunnel entrance, the freezing depth increased by 1m as the wind velocity increased from 1 m/s to 2 m/s, and the change in freezing depth was minimal as the wind velocity increased from 2 m/s to 3 m/s. In the center of the tunnel, the freezing depth increased by 2 m as the wind velocity increased from 1 m/s to 2 m/s, and the change in freezing depth was minimal as the wind velocity increased from 2 m/s to 3 m/s. At the exit, the freezing depth increased by 2 m and 1 m, respectively. At an outside air temperature of -15°C, as the wind velocity increased, at the tunnel entrance, the freezing depth increased by 1 m and 1 m, respectively,

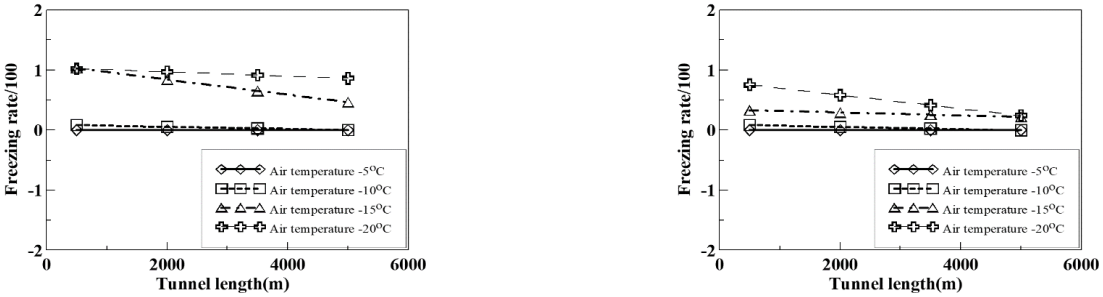

(a) One-way (b) Two-way

Fig. 20 Freezing rate according to the tunnel length

and at the tunnel center, the freezing depth increased by 2 m and 1 m, respectively. At the exit, the freezing depth increased by 3 m and 1 m. At an outside air temperature of -20°C, at the tunnel entrance, the freezing depth increased by 0 m and 1m, respectively, at the center, the freezing depth increased by 2 m and 1 m, respectively, and at the exit, the freezing depth increased by 3 m and 2 m, respectively. Fig. 17 displays Freezing depth according to the wind velocity.

5.1.3 Freezing rate and freezing depth according to tunnel diameter

(1) Internal Temperature of the Tunnel

The freezing rate of the tunnel, depending on the tunnel diameter, showed an increasing trend as the tunnel diameter increased, except when the outside temperature was -5℃. When the wind direction was one-way, the freezing rate was relatively lower compared to the two-way flow, and the increase in freezing rate was relatively smaller as the tunnel diameter increased.

When the outside temperature was -5℃, both one-way and two-way flows resulted in a freezing rate of 0% as the tunnel diameter increased. When the outside temperature was -10℃, the one-way flow exhibited a 20% increase in freezing rate when the tunnel diameter increased from 7 m to 11 m, while the two-way flow showed a 10% increase. With further increase in tunnel diameter to 15 m, the freezing rate increased to 31% and 8%, respectively. When the outside temperature dropped to -15℃, the one-way flow exhibited a 58% increase in freezing rate as the tunnel diameter increased from 7 m to 11 m, and a 100% freezing rate was observed for diameters larger than 11 m. In the case of two-way flow, the freezing rate increased by 12% and 6%, respectively, as the tunnel diameter increased. For an outside temperature of -20℃, the one-way flow resulted in a 27% increase in freezing rate as the tunnel diameter increased from 7 m to 11 m, and a 100% freezing rate was observed for diameters larger than 11 m. In the case of two-way flow, the freezing rate increased by 10% and 3%, respectively, as the tunnel diameter increased. Fig. 18 displays freezing rate according to the diameter.

(2) Tunnel ground

When air with below freezing temperature flowed in one-way or in two-way, the freezing depth of the ground material showed an increasing trend as the tunnel diameter increased.

In the case of one-way wind with a velocity of 2 m/s and a tunnel length of 5,000 m, when the outside temperature was -5℃, the freezing depth of the ground material increased as the tunnel diameter increased. At the tunnel entrance, the freezing depth was 1 m, 1 m in the middle section, and increased to 1 m at the exit, where the ground temperature remained above freezing until the tunnel diameter reached 15 m. When the outside temperature dropped to -10℃, at the tunnel entrance, an increase in tunnel diameter from 7 m to 11 m resulted in a 3 m increase in freezing depth, while an increase in diameter from 11 m to 15 m resulted in a 2 m increase. In the middle section, an increase in diameter from 7 m to 11 m led to a 3 m increase in freezing depth, and an increase from 11 m to 15 m resulted in a 2 m increase. At the exit, there was an increase of 2 m and 3 m in freezing depth, respectively. When the outside temperature reached -15℃, as the tunnel diameter increased, the entrance showed an increase of 3 m, 3 m, and the middle section showed an increase of 4 m, 4 m, while the exit had an increase of 3 m and 4 m in freezing depth. For an outside temperature of -20℃, at the entrance, the freezing depth increased by 4 m, 4 m, in the middle section it increased by 5 m, 5 m, and at the exit, it increased by 5 m, 5 m. Fig. 19 displays freezing depth according to the diameter.

5.1.4 Freezing rate and freezing depth according to tunnel length

(1) Internal Temperature of the Tunnel

When air with below freezing temperature flowed in one-way or in two-way, the freezing rate of the tunnel decreased progressively trend as the tunnel length increased, except when the outside temperature was -5℃. It was observed that the two-way flow resulted in relatively lower freezing rates compared to the one-way flow.

At a wind velocity of 1 m/s and a tunnel diameter of 11 m, when the outside temperature was -5℃, both one-way and two-way flows resulted in a freezing rate of 0%. When the outside temperature dropped to -10℃, both one-way and two-way flows exhibited freezing rates of 11% at a tunnel length of 500 m, 5% at 1,000 m, 2% at 3,000 m, and 1.7% at 5,000 m. For an outside temperature of -15℃, the one-way flow showed freezing rates of 100% at a tunnel length of 500 m, 100% at 1,000 m, 73% at 3,000 m, and 45% at 5,000 m. In the case of two-way flow, freezing rates of 33%, 31%, 27%, and 22% were observed, respectively. Furthermore, at an outside temperature of -20℃, the one-

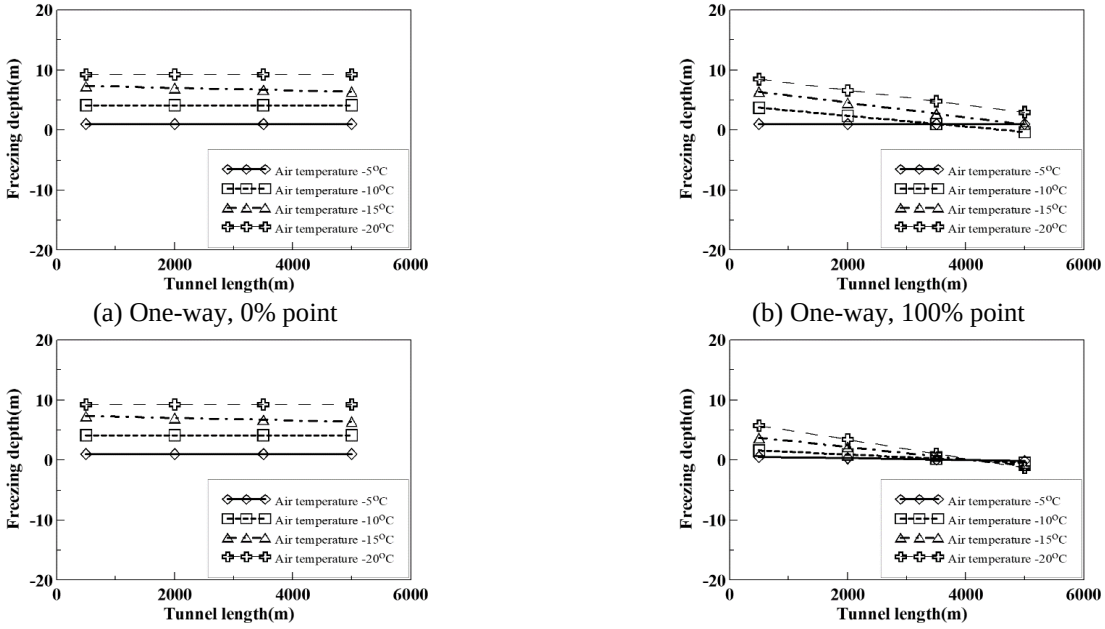

(a) One-way, 0% point (b) One-way, 100% point

(c) Two-way, 0% point (d) Two-way, 50% point

Fig. 21 Freezing depth according to the tunnel length

way flow exhibited a freezing rate of 100% up to a tunnel length of 3,000 m, and it decreased to 83% at a length of 5,000 m. In the case of two-way flow, a freezing rate of 100% was observed at a tunnel length of 500 m, and for tunnel lengths of 1,000 m, 3,000 m, and 5,000 m, freezing rates of 47%, 37%, and 32% were observed, respectively. Fig. 20 displays freezing rate according to the tunnel length.

(2) Ground of the tunnel

When air with below freezing temperature flowed in one-way or in two-way, the freezing depth of the ground, depending on the outside temperature, exhibited different patterns for the entrance, center, and exit sections of the tunnel. For the entrance section, both one-way and two-way flows showed consistent freezing depths as the tunnel length increased, except for a tunnel length of 5,000 m, where the freezing depth was different.

At the entrance section, for one-way and two-way flows, when the outside temperature was -5℃, a freezing depth of 1 m was observed across all tunnel lengths. When the outside temperature dropped to -10℃, a freezing depth of 4 m was observed. At an outside temperature of -15℃, a freezing depth of 7 m was observed for all tunnel lengths except for a length of 5,000 m, where it was 6 m. Furthermore, at an outside temperature of -20℃, a freezing depth of 9 m was observed for all tunnel lengths.

For the center section of the tunnel, in the case of one-way flow, when the outside temperature was -5℃, freezing depths of 2 m, 1 m, 1 m, and 0 m were observed for tunnel lengths of 500 m, 1,000 m, 3,000 m, and 5,000 m, respectively. When the outside temperature dropped to -10℃, freezing depths of 4 m, 4 m, 3 m, and 2 m were observed. At an outside temperature of -15℃, freezing depths of 7 m, 7 m, 5 m, and 4 m were observed, and at -20℃, freezing depths of 9 m, 9 m, 7 m, and 6 m were observed for all tunnel lengths.

For the exit section of the tunnel, when the outside temperature was -5℃, a freezing depth of 1 m was observed for all tunnel lengths, regardless of flow direction. When the outside temperature dropped to -10℃, freezing depths of 4 m, 3 m, 1 m, and 0 m were observed. At an outside temperature of -15℃, freezing depths of 6 m, 6 m, 3 m, and 1 m were observed, and at -20℃, freezing depths of 8 m, 8 m, 5 m, and 3 m were observed for each tunnel length.

In the case of two-way flow, between the entrance and center sections of the tunnel, when the outside temperature was -5℃, a freezing depth of 1 m was observed for tunnel lengths of 500 m and 1,000 m, while 0 m freezing depth was observed for tunnel lengths of 3,000 m and 5,000 m. When the outside temperature dropped to -10℃, freezing depths of 3 m, 3 m, 2 m, and 2 m were observed. At an outside temperature of -15℃, freezing depths of 6 m, 6 m, 5 m, and 4 m were observed, and at -20℃, freezing depths of 8 m, 8 m, 7 m, and 6 m were observed for each tunnel length. For the center section of the tunnel, when the outside temperature was -5℃, a freezing depth of 1 m was observed only for a tunnel length of 500 m, while 0 m freezing depth was observed for longer tunnel lengths. When the outside temperature dropped to –10℃. Fig. 21 displays Freezing depth according to the tunnel length.

5.2 Freezing range prediction model through multiple regression analysis

5.2.1 Estimation equation for lengthwise freezing rate of the tunnel

In this study conducted multiple regression analysis to derive a regression equation that can estimate the freezing rate inside the tunnel based on the freezing rate calculated according to the structural and environmental conditions of the tunnel.

The independent variables considered in the numerical

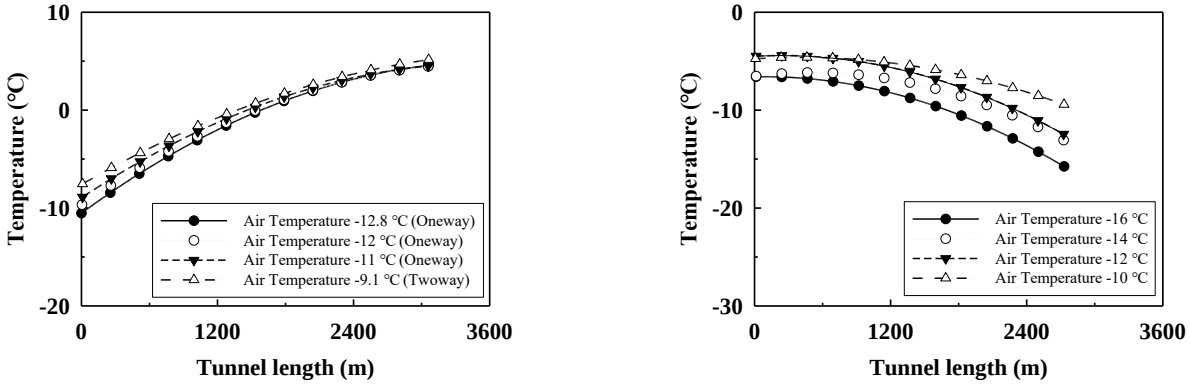

(a) ○○ Tunnel (b) Zuomutai Tunnel

Fig. 22 Results of internal temperature measurement

analysis were the tunnel diameter, tunnel length, ambient temperature, and wind velocity. The freezing rate was considered as the dependent variable, and the following Eq. (5) was selected as the regression model. Subsequently, the coefficients and constants for the independent variables were determined, and regression equations for estimating the freezing rate in the lengthwise direction of the tunnel ($F_{R,one}$) when the wind direction is one-way and in the lengthwise direction of the tunnel ($F_{R,two}$) when the wind direction is two-way were derived.

$$F = a_1 D + a_2 L + a_3 w + a_4 T + b \quad (5)$$

$$F_{R,one}(\%) = 2.82D - 0.004L + 11.67w + 6.47T - 65.93 \quad (6)$$

$$F_{R,two}(\%) = 2.56D - 0.007L + 10.11w + 4.5T - 52.35 \quad (7)$$

Where D is the tunnel diameter, L is the tunnel length, w is the wind velocity, T is the air temperature.

5.2.2 Estimation equation for ground freezing depth of the tunnel

In this study performed multiple regression analysis to derive a regression equation that can estimate the freezing depth of the tunnel's ground under different conditions, based on the freezing depth calculated according to the structural and environmental conditions of the tunnel.

The independent variables are the same as those used for estimating the lengthwise freezing rate, and the dependent variable is the freezing depth. We selected the regression model represented by Eq. (5). Subsequently, by determining the coefficients and constants for the independent variables, regression equations were derived to estimate the ground freezing depth at the entrance ($F_{D,one,0\%}$), the middle section ($F_{D,one,50\%}$), and the exit ($F_{D,one,100\%}$) of the tunnel when the wind direction is one-way, as well as at the entrance ($F_{D,two,0\%}$), between the entrance and the middle section ($F_{D,two,25\%}$), and the middle section ($F_{D,two,50\%}$) when the wind direction is two-way.

$$F_{D,one,0\%}(m) = 0.64D - 0.0001L + 0.48w + 0.53T - 8.47 \quad (8)$$

$$F_{D,one,50\%}(m) = 0.68D - 0.0004L + 0.82w + 0.5T - 9.01 \quad (9)$$

$$F_{D,one,100\%}(m) = 0.67D - 0.0006L + 1.01w + 0.45T - 8.99 \quad (10)$$

$$F_{D,two,0\%}(m) = 0.61D - 0.0001L + 0.49w + 0.53T - 8.16 \quad (11)$$

$$F_{D,two,25\%}(m) = 0.65D - 0.0003L + 0.96w + 0.49T - 9.47 \quad (12)$$

$$F_{D,two,50\%}(m) = 0.47D - 0.0012L + 0.74w + 0.22T - 4.22 \quad (13)$$

Where F_D is the freezing depth.

5.3 Validation of regression equation

To validate the regression equation for predicting the tunnel freezing range presented earlier, the freezing rates of the tunnel derived from field measurements and those calculated using the regression equation were compared and analyzed. The validation of the regression equation involved analyzing the field measurement results through regression analysis and determining the segments where the internal temperature of the tunnel falls below -7°C to calculate the freezing rates of the tunnel. The calculated freezing rates obtained from the regression equation were then quantitatively compared with those obtained from the field measurements. However, due to the rarity of field measurement cases for the freezing depth of the tunnel backfill, they were excluded from the analysis.

The field measurement data utilized in this study were obtained from temperature measurements inside tunnels located in cold regions both domestically and internationally. The selected tunnels for measurement included the ○○ Tunnel in Korea and the Zuomutai Tunnel in China.

The ○○ Tunnel is designed as a very long tunnel with a width of 11 meters, a height of 7.8 meters, and a length of 8,293 meters. Temperature measurements were taken longitudinally from the tunnel entrance to the midpoint at 3,270 meters. The measurement intervals were set at 30-meter increments from the portal to 210 meters, followed by increments of 50 meters, 70 meters, and 90 meters.

Table 5 Calculated freezing rates of OO Tunnel

OO Tunnel				Freezing rate(%)		
				Field measurement	Regression equation	Error
Wind direction	Oneway	Air temperature (℃)	-11	3.17	2.5	0.67
			-12	4.27	9	-4.73
			-12.8	5.27	14.11	-8.84
	Twoway		-9.1	1.1	0	1.1

Table 6 Calculated freezing rates of Zuomutai Tunnel

Zuomutai Tunnel				Freezing rate(%)		
				Field measurement	Regression equation	Error
Wind direction	Oneway	Air temperature (℃)	-10		30.21	-3.39
			-13	38	43.15	-5.15
			-13.6	57.14	53.50	3.64
			-16.4	75	71.62	3.38

The Zuomutai Tunnel is a road tunnel located on the Hegang-Dalian Expressway, known for its monthly average minimum temperature of -16.1°C. The tunnel has a height of approximately 7.1 meters and a length of 2,910 meters. Wind velocity typically range from 1 m/s to 3 m/s in summer and consistently remain above 2 m/s during winter.

The calculation of the freezing rate through field measurements in the ○○ Tunnel showed a freezing rate ranging from 3.17% to 5.27% at an outside temperature range of -11°C to -12.8°C when the wind direction was oneway. Meanwhile, the freezing rate calculated through regression analysis ranged from 2.5% to 14.11%, indicating an average error of 4.74%. In the case of twoway wind direction, field measurements showed a freezing rate of 1.1%, whereas the regression analysis indicated a freezing rate of 0%.

In the case of the Zuomutai Tunnel, on-site measurements showed a freezing rate ranging from 26.82% to 75% at an outside temperature range of -10°C to -16.4°C. Additionally, regression analysis indicated a freezing rate ranging from 30.21% to 71.62%. The average error between field measurements and regression analysis was 3.89%.

Therefore, the regression equations proposed in this study are considered to relatively accurately simulate the freezing rate along the tunnel's longitudinal direction, and they are deemed applicable for estimating the freezing rate of tunnels based on their environmental and structural conditions.

Fig. 22 presents the internal temperature measurement results of ○○ Tunnel and Zuomutai Tunnel in graphical form, while Table 5 and 6 present the calculated freezing rates based on field measurements and regression analysis for ○○ Tunnel and Zuomutai Tunnel, respectively.

6. Conclusions

This study focused on the numerical analysis of freezing range in cold regions tunnels. Three-dimensional heat transfer numerical analysis was conducted to analyze the freezing range of tunnels in cold regions. Regression analysis was performed using the results of the numerical analysis to derive estimation equations for freezing rate and freezing depth, providing insights into the freezing range of tunnels. In summary, the conclusions of this paper are as follows.

(1) To validate the model before conducting numerical analysis to examine the temperature distribution inside the tunnel, as well as the lining and ground, a comparison and analysis were performed between the results of numerical analysis considering the field measurement results and the site conditions. The results showed an average error of approximately 0.09℃ and a correlation coefficient of 0.98, indicating a very high correlation between the field measurements and the numerical analysis. Therefore, it was concluded that the numerical analysis model for verifying the temperature distribution inside the tunnel and the lining and ground is valid.

(2) Considering the structural and environmental conditions of the tunnel, the thermal analysis results showed that the temperature distribution inside the tunnel exhibited a gradual increase from the entrance to the exit when the wind direction was one-way. When the wind direction was two-way, the temperature gradually increased from the entrance to the center and decreased symmetrically towards the exit. The temperature distribution of the ground in the tunnel showed that as the depth increased from the lining surface to the ground, the temperature gradually approached the underground temperature, both when the wind direction was one-way and two-way. Particularly in tunnels with

relatively long extensions under two-way wind conditions, the temperature of the ground at the center of the tunnel remained close to the underground temperature. Therefore, the internal temperature of the tunnel and the temperature of the ground exhibit different trends depending on the wind direction, indicating that the freezing range of the tunnel should be differentiated according to the wind direction.

(3) The numerical analysis results showed that the internal temperature of the tunnel and the temperature of the ground decrease as the external temperature decreases and increase as the wind velocity increases under environmental conditions. Furthermore, under the structural conditions of the tunnel, the internal temperature of the tunnel and the temperature of the ground decrease as the tunnel diameter increases. It has been confirmed that as the length of the tunnel increases, the segment where the temperature above-zero is maintained also increases. Therefore, in the design of tunnels in cold regions, careful consideration should be given to environmental conditions such as low external temperatures and high wind velocity, and tunnels with smaller cross-sections are advantageous in terms of freezing prevention. For tunnels with shorter lengths, freezing prevention measures should be implemented throughout the entire length.

(4) Regression analysis was performed based on the analysis conditions using the results of the numerical analysis to estimate the lengthwise freezing rate of the tunnel and the freezing depth of the ground. The derived regression equations allow the estimation of the freezing rate and freezing depth of the tunnel's lengthwise direction and the ground, considering the structural and environmental conditions of the tunnel according to the wind direction. Therefore, it is deemed that the derived regression equations can be used to determine the freezing range of the tunnel's lengthwise direction and the freezing range of the ground based on the structural and environmental conditions of the tunnel, considering the wind direction.

(5) In conclusion, the freezing range of tunnels in cold regions should be determined by considering the tunnel diameter, length, wind velocity, and external temperature. The numerical analysis model used in this study can be utilized for further examination, and it is deemed that additional research on the refinement of the regression equations for estimating the freezing range of the tunnel through Transient analysis, considering variables that change over time, will be necessary in the future.

Acknowledgments

The research described in this paper was financially supported by the National Research Foundation of Korea (NRF) grant funded by the Korean government (MSIT) (NRF-2021R1I1A3056148).

References

An, J.W. (2020), "A study on the freeze-thaw characteristics and quantitative evaluation nethod for concrete lining of mountain tunnel in winter season", Ph.D. Dissertation, Kyungpook National University, Daegu, South Korea.

Broch, E., Grøv, E. and Davik, K.I. (2002), "The inner lining system in Norwegian traffic tunnels", *Tunn. Undergr. Sp. Tech*., **17**(3), 305-314. https://doi.org/10.1016/S0886-7798(02)00026-3.

Cui, G. and Wang, X. (2021), "Engineering application and study on polyurethane-corrugated steel plate insulation lining of existing railway tunnel in seasonal frozen area", *Sci. Progress*, **104**(1), 1-17. https://doi.org/10.1177/0036850420987043.

Hwang, Y.C. (2013), "Maintenance characteristics of geotechnical structures in cold region for freeze damage analysis", *J. Korean Geo-Environ. Soc.*, **14**(3), 35-40. UCI :G704-SER000001652.2013.14.3.001.

Jumassultan, A., Sagidullina, N., Kim, J., Ku, T. and Moon, S, W. (2021), "Performance of cement-stabilized sand subjected to freeze-thaw cycles", *Geomech. Eng*., **25**(1), 41-48. https://doi.org/10.12989/gae.2021.25.1.041

Jin, H.J., Lee, J.G. and Ryu, B,H. (2022), "Investigation of the ASTM International frost heave testing method using a temperature-controllable cell", *Geomech. Eng*., **31**(6), 583-597. https://doi.org/10.12989/gae.2022.31.6.583.

Jun, K.J. (2019), "Analysis of factors affecting the internal temperature in road tunnels located in cold regions and development of an estimation model", Ph.D. Dissertation, Gangneung-Wonju National University, Gangneung, South Korea.

Kang, H.C., Kang, B.H., Kim, S.H. and Jung, M. (2013), "Heat transfer in practice", Sci. Tech, Seoul, South Korea.

KDS 27 00 00 (2018), Tunnel Design Standard, Korea Construction Standards Center, Goyang, South Korea.

KDS 27 10 10 (2016), Tunnel Design Standard, Investigation and Planning, Korea Construction Standards Center, Goyang, South Korea.

KDS 27 50 05 (2016), Tunnel Design Standard, Drainage and Waterproofing, Korea Construction Standards Center, Goyang, South Korea.

Kim, D.Y., Lee, H.S. and Sim, B.K. (2011), "A study on the design of tunnel lining insulation based on measurement of temperature in tunnel", *Korean Tunneling and Underground Space Association*, **13**(4), 319-345. UCI: G704-001074.2011.13.4.001.

Korea Expressway Corporation (2006), "Review of anti-icing measures for tunnel drainage facilities", Korea Expressway Corporation, Gimcheon, South Korea.

Korea Expressway Corporation (2013), "A Study on the antifreeze of concrete lining according to the temperature drop in the tunnel", Korea Expressway Corporation, Gimcheon, South Korea.

Ma, Q., Luo, X., Lai, Y., Niu, F. and Gao, J. (2018), "Numerical investigation on thermal insulation layer of a tunnel in seasonally frozen regions", *Appl. Therm. Eng*., **138**, 280-291. https://doi.org/10.1016/j.applthermaleng.2018.04.063.

Ministry of Land, Infrastructure and Transport (2020), "Railway tunnel status by year", Ministry of Land, Infrastructure and Transport, Sejong, South Korea.

Ministry of Land, Infrastructure and Transport (2020), "Road bridge and tunnel status report", Ministry of Land, Infrastructure and Transport, Sejong, South Korea.

Moon, J.S., An, J.W., Kim, H.K., Lee, J.G. and Tim, L. (2022), "Evaluation criteria for freezing and thawing of tunnel concrete lining according to theoretical and experimental analysis", *Geomech. Eng*., **29**(3), 349-357, https://doi.org/10.12989/gae.2022.29.3.349.

Park, Y.S., Lee, S.H. and Cho, K.H. (2021), "Temperature Distribution of Railway Tunnels in Winter", *J. Korean Soc. Hazard Mitig*., **21**(1), 199-205. https://doi.org/10.9798/KOSHAM.2021.21.1.199.

Park, S,.Y., Hwang, C.M., Choi, H.S., Son, Y.J. and Ko, T.Y.

(2022), "Experimental study for application of the punch shear test to estimate adfreezing strength of frozen soil-structure interface", *Geomech. Eng.*, **29**(3), 281-290, https://doi.org/10.12989/gae.2022.29.3.281.

Son, H.S., Jun, K.J. and Yune, C.Y. (2017), "Analysis on Freezing Reduction of Road Tunnels with Heat Insulation Method during Winter", *J. Korean Geotech. Soc*., **33**(8), 17-27. https://doi.org/10.7843/kgs.2017.33.8.17.

Tao, L., Tian, X., Zhou, X. and Zeng, Y. (2022a), "Influence of mechanical wind heated by ground temperature on ambient temperature in tunnels: Numerical modeling, case study and analysis", *Int. J. Therm. Sci*., **176**, 107497. https://doi.org/10.1016/j.ijthermalsci.2022.107497.

Tao, L., Zhou, X., Tian, X., Ye, X., Zeng, Y. and Liu, X. (2022b), "Study on the temperatures of railway tunnel side ditches in high-latitude cold regions based on the effects of wind", *Case Stud. Therm. Eng*., **30**, 101793. https://doi.org/10.1016/j.csite.2022.101793.

TSNE (2020), "Ansys 2020 R1 Mechanical", Sigmapress, Seoul, South Korea.

Wu, H., Zhong, Y., Xu, W., Shi, W., Shi, X. and Liu, T. (2020), "Experimental investigation of ground and air temperature fields of a cold-region road tunnel in NW China", *Adv. Civil Eng*., **2020**, 4732490. https://doi.org/10.1155/2020/4732490.

Zhao, P., Chen, J., Luo, Y., Li, Y., Chen, L., Wang, C. and Hu, T. (2020), "Field measurement of air temperature in a cold region tunnel in Northeast China", *Cold Reg. Sci. Tech*., **171**, 102957. https://doi.org/10.1016/j.coldregions.2019.102957.

Zhou, X., Zeng, Y. and Fan, L. (2016), "Temperature field analysis of a cold-region railway tunnel considering mechanical and train-induced ventilation effects", *Appl. Therm. Eng*., **100**, 114-124. https://doi.org/10.1016/j.applthermaleng.2016.01.070.

GC